FACULDADE DE ENGENHARIA DA UNIVERSIDADE DO PORTO

Evaluation of Wi-Fi Underwater Networks in Freshwater

Pedro Manuel Cadavez Pacheco Carneiro de Freitas

FOR JURY EVALUATION

MESTRADO INTEGRADO EM ENGENHARIA ELETROTÉCNICA E DE COMPUTADORES

Advisor: Prof. Manuel Alberto Pereira Ricardo (PhD)

Co-Advisor: Eng. Filipe Borges Teixeira (MSc)

July 31, 2014

U.PORTO

FEUP FACULDADE DE ENGENHARIA UNIVERSIDADE DO PORTO

MIEEC - MESTRADO INTEGRADO EM ENGENHARIA ELETROTÉCNICA E DE COMPUTADORES 2013/2014

A Dissertação intitulada

"Evaluation of Wi-Fi Underwater Networks in Freshwater"

foi aprovada em provas realizadas em 15-07-2014

o júri

Presidente Professor Doutor Sílvio Almeida Abrantes Moreira
Professor Auxiliar do Departamento de Engenharia Eletrotécnica e de Computadores da Faculdade de Engenharia da Universidade do Porto

Professor Doutor Jorge Botelho da Costa Mamede
Professor Adjunto do Departamento de Engenharia Eletrotécnica do Instituto Superior de Engenharia do Porto

Professor Doutor Manuel Alberto Pereira Ricardo
Professor Associado do Departamento de Engenharia Eletrotécnica e de Computadores da Faculdade de Engenharia da Universidade do Porto

O autor declara que a presente dissertação (ou relatório de projeto) é da sua exclusiva autoria e foi escrita sem qualquer apoio externo não explicitamente autorizado. Os resultados, ideias, parágrafos, ou outros extratos tomados de ou inspirados em trabalhos de outros autores, e demais referências bibliográficas usadas, são corretamente citados.

Autor - Pedro Manuel Cadavez Pacheco Carneiro de Freitas

Faculdade de Engenharia da Universidade do Porto

© Pedro Freitas, 2014

Abstract

Underwater wireless communications are receiving an increasing interest in the past years. Applications such as environmental observation, oil/gas facilities monitoring or oceanographic data using remotely operated vehicles require new communication solutions that are able to achieve high data rate links and low acquisition and maintenance costs. Current solutions for underwater scenarios rely on acoustic and optical technology that may be only suitable for some scenarios. While optical solutions may already achieve high data rates at low distances, its related costs and severe limitations, such as the need of line-of-sight and strong disturbance caused by sun light, makes this technology unattractive. Radio frequency (RF) based communications may have an important role in this matter. Although associated with shorter ranges due to the high conductivity of water, it is possible to achieve data rates greater than the offered by acoustic solutions. Using RF devices with IEEE 802.11 Standards may allow to achieve a low cost solution for short range high data rate underwater communications.

This dissertation aims at designing a testbed for an underwater environment and evaluate the performance of IEEE 802.11 networks at 700 MHz, 2.4 GHz and 5 GHz when applied to underwater scenarios. A new antenna for 768 MHz was designed and tested, providing an increase of 50% on the maximum communication range, comparing to an air adapted antenna for the same frequency.

Experimental results at the different frequencies are promising, emphasized with the achievement of more than 2 meters communication range using the 768 MHz frequency with data rates in the order of 400 kbit/s and a minimum of 11 Mbit/s for distances lower than 1.6 meters. Frequencies in the 2.4 and 5 GHz bands show maximum communication ranges of 32 and 10 cm, respectively. High data rates were accomplished for distances lower than 20 cm at 2.462 GHz, reaching more than 100 Mbit/s of throughput, and at 5 GHz 10 Mbit/s at a 10 cm distance. These results provide a validation and prove feasibility on the use of RF technology for wide band underwater communications.

Resumo

As comunicações subaquáticas sem fios têm recebido um interesse crescente nos últimos anos. Aplicações como observação ambiental, monitorização de estruturas da indústria do petróleo/gás e recolha de dados oceanográficos usando veículos operados remotamente requerem novas soluções capazes de atingir comunicações de elevados débitos e custos de aquisição e manutenção reduzidos. As soluções atuais dependem das tecnologias acústicas e óticas que poderão ser adequadas para apenas alguns cenários. Enquanto as soluções óticas podem já atingir elevados débitos a curtas distâncias os custos associados e severas limitações, como a necessidade de linha de vista e a elevada perturbação causada pela luz solar, tornam esta tecnologia pouco atrativa. Comunicações baseadas em radio frequência poderão ter um importante papel nesta matéria. Apesar de associadas a curtas distâncias devido à elevada condutividade da água, é possível atingir débitos superiores aos oferecidos pelas soluções óticas. O uso de dispositivos de rádio frequência com normas IEEE 802.11 podem permitir alcançar uma solução de baixo custo para comunicações subaquáticas de curto alcance.

Esta dissertação tem como objetivo desenvolver um *testbed* para um ambiente subaquático e avaliar a performance de redes IEEE 802.11 nas bandas de frequência de 700 MHz, 2.4 GHz e 5GHz. Uma nova antena para 768 MHz foi desenvolvida e testada, proporcionando um aumento de 50% no alcance máximo de comunicação, comparando a uma antena adaptada ao ar para a mesma frequência.

Resultados experimentais nas diferentes frequências são promissores, realçados por ter sido atingida uma distância de comunicação superior a 2 metros na frequência de 768 MHz com débitos na ordem dos 400 kbit/s e um mínimo de 11 Mbit/s para distâncias inferiores a 1.6 metros. Frequências nas bandas de 2.4 e 5 GHz mostram alcances máximos de 32 e 10 cm, respetivamente. Elevados débitos foram alcançados para distâncias inferiores a 20 cm a 2.462 GHz, com débitos superiores a 100 Mbit/s, e a 5 GHz 10 Mbit/s a 10 cm de distância. Estes resultados fornecem a validação e provam a viabilidade do uso da tecnologia radio frequência para comunicações subaquáticas de banda larga.

Acknowledgments

First of all, i would like to thank my parents and closest family for providing me the means to attend university. Regarding my dissertation, i would like to thank my advisor, Prof. Manuel Ricardo for giving me the opportunity of joining this challenging project. Also, to my co-advisor, Filipe Teixeira, and Rui Campos for all the guidance and patience. Another big contribution was giving from Mário Lopes, Luis Pessoa e Mário Pereira, for sharing their knowledge. I would to also thank ISEP, for providing the facilities required to perform this dissertation experiments.

This would not be possible to accomplish without the support of my brothers, friends and specially Vânia.

Finnaly, i would like to thank the BEST CASE project (“NORTE-07-0124-FEDER-000058” and "NORTE-07-0124-FEDER-000060") financed by the North Portugal Regional Operational Programme (ON.2 – O Novo Norte), under the National Strategic Reference Framework (NSRF), through the European Regional Development Fund (ERDF), and by national funds, through the Portuguese funding agency, Fundação para a Ciência e a Tecnologia (FCT).

Pedro Cadavez de Freitas

"There is no great genius without a mixture of madness."

Aristotle

Contents

List of Figures

List of Tables

Abbreviations

ACK	Acknowledge
BPSK	Binary Phase Shift Keying
CCK	Complementary Code Keying
CSMA/CA	Carrier Sense Multiple Access / Collision Avoidance
CTS	Clear to Send
DBPSK	Differential Binary Phase Shift Keying
DQPSK	Differential Quaternary Phase-Shift Keying
DSSS	Direct sequence spread spectrum
EM	Electromagnetic
EMI	Electromagnetic Interference
EWMA	Exponentially-Weighted Moving Average
FHSS	Frequency Hopping spread spectrum
HR-DSSS	High-Rate Direct sequence spread spectrum
HT	High Throughput
HTTP	HyperText Transfer Protocol
IEEE	Institute of Electrical and Electronics Engineers
INESC TEC	INstituto de Engenharia de Sistemas e Computadores - Tecnologia e Ciência
ISM	Industrial, Scientific and Medicine
LAN	Local Area Network
LED	Light-emitting diode
MAC	Media Access Control
MAN	Metropolitan Area Network
MIMO	Multiple Input Multiple Output
OFDM	Orthogonal frequency division multiplexing
PHY	Physical Layer
POE	Power Over Ethernet
RAA	Rate Adaptation Algorithms
RF	Radio Frequency
RTS	Ready to Send
RTT	Round Trip Time
SSH	Secure Shell
UW	Underwater
VLF	Very Low Frequency
WLAN	Wireless Local Area Network

Chapter 1

Introduction

1.1 Context

Wireless communications have been subject of enormous research and improvements in the near past. This effort is responsible for allowing multiple devices to securely communicate simultaneously with high availability, great distances and high data rates. While these improvements are applied and tested mainly in over-the-air communications, underwater communications suffer from a low applicability of RF transmission systems due to electromagnetic waves attenuation in water [1].

The significant interest in underwater communications comes due to a wide range of applications including coastline protection, underwater environmental observation for exploration, offshore oil/gas field monitoring, oceanographic data collection, autonomous underwater vehicles (AUVs) and remotely operated vehicles (ROVs) [1]. Local economies and environment can also benefit from data monitoring and transmission in shallow fresh water since they may provide crucial information.

When using radio frequency, underwater communications do not fully benefit from the improvements achieved in air since electromagnetic propagation in water causes a big reduction in the effective range. Because of the limitations that water imposes, these communications are currently performed using acoustic waves and in some cases optical systems. Acoustic technology generally provides low transmission rates and the use of expensive equipments. While optical systems may achieve high data rates, these are also associated with expensive equipments and maintenance, and may be severely limited by line-of-sight and sun light, if at shallow water. Wi-Fi based communications may allow the use of a low cost technology in short range freshwater scenarios at higher data rates when comparing with acoustic/optical solutions.

1.2 Motivation

As current solutions for underwater communications may not fulfill the requirements for some present or incoming applications, it is crucial to find a solution that does. Acoustic and optical systems have, in general, proprietary designs that are associated with high design and maintenance costs. Saying this, Wi-Fi has the potential to provide an ideal solution for certain applications, where high data rate transmission is required at short distances. As with performance needs, equipment and maintenance costs are a big concern. Because Wi-Fi devices are globally available, their cost is relatively low to other solutions. Also, having into account that these devices are used to provide wireless communications everywhere like homes, offices, companies and open spaces, knowledge on how to handle them comes almost from common sense. This can be considered for low maintenance costs. Another contribution for Wi-Fi low cost is the use of frequencies that are part of the unlicensed ISM (industrial,scientific and medicine) radio bands, meaning that there are no costs for using these frequencies. ISM radio bands are portions of the radio spectrum reserved internationally for the use of RF energy for industrial, scientific and medical. In spite of the real purpose of ISM bands, there has been rapid growth in its use in low-power, short-range communications platforms.

1.3 Objectives

The goal of this dissertation is to study the performance of Wi-Fi communications in freshwater scenarios. To achieve this, a testbed will be designed and optimized to work in an underwater environment. Underwater experiments will be carried inside a tank with 10m per 6m area and a 5m depth. The performance of the system will be tested using 700 MHz, 2.4 GHz and 5 GHz band frequencies, as for automatic rate adaptation and its applicability to underwater communications. The objectives will be divided as followed:

- Study of the performance considering:
  - **First Phase**: two submerged nodes at different frequencies and distances;
  - **Second Phase**: three submerged nodes competing for the same medium, for medium access control mechanisms evaluation.
- Analysis and comparison between experimental results and the ones provided by theoretical propagation models;

1.4 Results

The main contributions of this dissertation are summarized as following:

- **Design of a testbed for Underwater Wi-Fi communications evaluation** - A setup was developed in order to evaluate IEEE 802.11 networks underwater. The implemented testbed provided reliable data and supplied a versatile solution for various scenarios.
- **Design and characterization of a new antenna for an underwater environment at 768 MHz** - A new antenna was designed that provides an improvement in at least 40% on efficiency of the transmission power, resulting in an increase of 50% on the maximum communication range.
- **Experimental analysis of IEEE 802.11 networks at 700 MHz, 2.4 GHz and 5 GHz performance** - Throughput, jitter, round trip time and RSSI was measured for the different frequencies and results were understood.

Experiments results showed more than 2 meters communication range using the 768 MHz frequency with data rates in the order of 400 kbit/s and a minimum of 11 Mbit/s for distances lower than 1.6 meters. Frequencies in the 2.4 and 5 GHz bands show maximum communication ranges of 32 and 10 cm, respectively. High data rates were accomplished for distances lower than 20 cm at 2.462 GHz, reaching 100 Mbit/s of throughput, and at 5 GHz 10 Mbit/s at a 10 cm distance.

In our Multiple Access evaluation, the Hidden Node problem manifested, reducing communications performance. RTS/CTS mechanism may diminish this effect.

1.5 Structure

This document is divided in 4 Chapters. In Chapter 2 we describe the state of the art. Chapter 3 describes the design and optimization of the testbed. In Chapter 4 we provide the results and discussion of the experiences. Chapter 5 presents the final conclusions and future work.

Chapter 2

State of The Art

In this chapter, we overview underwater communications systems. The applicability of each system and their limitations are explored in order to compare them. In addition, a propagation model for RF communications is discussed and applied to the 700 MHz, 2.4 GHz and 5 GHz frequencies so that theoretical results can be compared to the practical experiments. IEEE 802.11 standards are comprehended in order to understand how its specifications may affect underwater communications.

2.1 Underwater Wireless Communications

Underwater wireless communications research is focused on the use of acoustic, optical and electromagnetic signals. The variety of systems available reflect the strong performance dependence to the limitations of the medium. Each system configuration and technique provide solutions for specific applications, where a trade-off between range and data rate is a standard. While some improvements have been seen using acoustic and optical technologies, radio frequency communications have not been subject for many works or investments.

2.1.1 Acoustic

Acoustic waves are produced from variations of pressure in a medium. They travel 4-5 times faster in water than they do in air, due to the greater density of water [2]. The speed of sound in water is about 1500 m/s, while traveling at 340 m/s in air. The propagation speed thought, is highly dependent on the temperature, pressure and salinity of the water. These can be responsible for drastically changing the direction of the sound is moving in, or even make it propagate through longer distances [3].

Underwater acoustic communications are generally recognized as one of the most difficult communication media in use today. Acoustic propagation is best supported at low frequencies, and the bandwidth available for communication is extremely limited. An acoustic system may operate in a frequency range between 10 and 15 kHz [4], having a very low total communication bandwidth of 5 kHz. The system is although ultra-wideband, meaning that bandwidth is not

negligible with respect to the center frequency. A survey of acoustic systems commercialized at the present are shown in Table 2.1.

Table 2.1: Commercialized acoustic modems specifications

Model	Distance(m)	Rate (kbit/s)	Operating Frequency(kHz)	Power (Watts)	Depth (m)
LinkQuest UWM1000	350	9.6 to 19.2	26.77 to 44.62	2	Up to 200
LinkQuest UWM2000	1500	9.6 to 19.2	26.77 to 44.62	8	Up to 4000
LinkQuest UWM3000	5000	2.5 to 5	7.5 to 12.5	12	Up to 7000
LinkQuest UWM4000	4000	4.8 to 9.6	12.75 to 21.25	7	Up to 7000
LinkQuest UWM10000	10000	2.5 to 5	7.5 to 12.5	40	Up to 7000
EvoLogics S2CR 48/78	1000	31.2	48 to 78	60	Up to 2000
EvoLogics S2CR 42/65	1000	31.2	42 to 65	60	Up to 2000
EvoLogics S2CR 18/34	3500	13.9	18 to 34	80	Up to 2000
EvoLogics S2CR 7/17	8000	6.9	7 to 17	80	Up to 6000

As shown in Table 2.1, the fastest acoustic modem can only transmit at 31.2 kbit/s at a 1000m distance, while the one with the longer distance (10 km) can transmit at 5 kbit/s Although attractive distances are achieved, these data rates may only be suitable to transmit basic control signals or small messages, making acoustic communications impossible to be used by applications that require larger data exchanges, like live audio or video. The good propagation of sound in water also contributes to the big sensitivity these systems have to acoustic "noise" from other sources. Shallow water reflections and attenuation, the poor performance in shadow water and the sensitivity to environmental characteristics are also major limitations factors [3]. Acoustic waves can also be adversely affected by spreading loss, and severe multi-path [2]. Low speed propagation implies high latency for long range, that is critical to real-time response synchronization and multiple-access protocols.

Although acoustic modems may have their uses in particular scenarios, namely in distances over 1 km, acoustic wireless transmission is not feasible when high data rates even if at short distances are required.

2.1.2 Optical

Optical communications are performed using light to carry information. Light is an electromagnetic wave, and so, shares the same characteristics from RF waves, but having a higher frequency (430–790 THz). As shown in Figure 2.1, visible light frequencies are the least attenuated in all of electromagnetic radiation. Wavelengths in the 470 nm range are, in general, attenuated the least, always depending on the characteristics of the specific water, since absorption and scattering is influenced by the chemical and biological make up of the water [3]. The low attenuation at these frequencies and the high propagation speed of electromagnetic waves provide optical systems the possibility to communicate at data rates highly superior to the acoustic systems. Figure 2.2 shows

that the blue light is the least attenuated, and so, used by many commercial systems and research experiments.

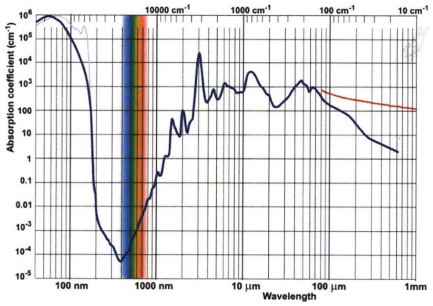

Figure 2.1: Absorption coefficient of electromagnetic radiation at various wavelengths [3]

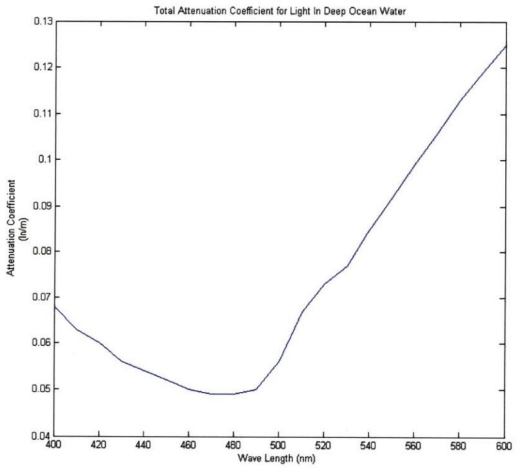

Figure 2.2: Absorption coefficients of visible light wavelengths [3].

Its limitations rely on the fact that light, being an electromagnetic wave, it is strongly attenuated in water, which compromises the transmission range. These limitations are better discussed in Chapter 2.1.3. An intrinsic limitation of optical systems is the strong dependence on line-of-sight which can be challenging when considering an underwater environment. Recent improvements in LED technology [5] have enabled low cost, power efficient optical transmitters to be developed that offer high level of light intensity, fast switching speeds, high efficiency, and optimal wavelengths for underwater light transmissions. The use of lasers instead of LEDs can improve even further the quality of the transmission since it provides a much better collimated light beam than LED. However it is much more susceptible to misalignment and so, not always considered [5].

Despite acoustic systems may provide suitable underwater communications because sound propagates well in water, optical systems may be better solution when the application requires higher data rate at the cost of effective range [5]. As we can see from the survey of commercial Optical Systems shown in Table 2.2, some systems achieve data rates in the Mbit/s order, a lot more than the data rates provided by acoustic systems. Nevertheless, the need for line-of-sight and the strong reduction of performance caused by scattering, makes these systems impossible to apply in some scenarios. Two examples of optical systems are shown in Figure 2.3.

Table 2.2: Commercialized optical modems specifications

Model	Distance(m)	Rate	Operating Frequency	Max. Depth
AQUAmodem 500	250	25 – 100 bit/s	27 – 31 kHz	200
AQUAmodem Op1	1	19.20 kbit/s	610 – 575 THz (cyan)	3000
NEPTUNE (SA Photonic)	10 - 200	10 - 250 Mbit/s	532 nm / 486 nm	N/A
1013C1 (Ambalux)	up to 40	10 Mbit/s	N/A	60

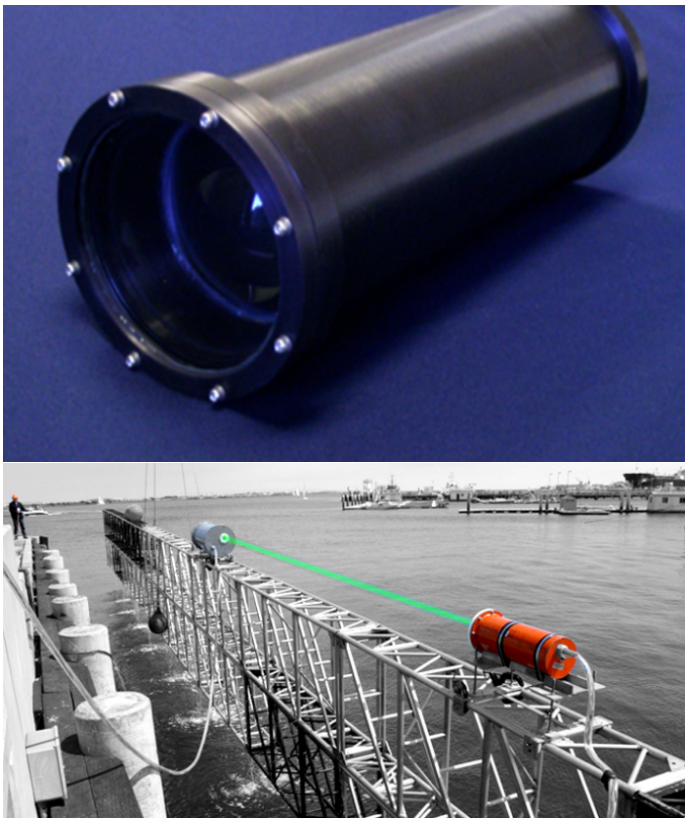

Figure 2.3: Examples of Optical Systems (1013C1 (Ambalux) and NEPTUNE (SA Photonic))

2.1.3 Radio frequency

Radio frequency waves are electromagnetic waves in the frequency band below 300 GHz. An electromagnetic wave is a wave of energy having a frequency within the electromagnetic spectrum (Figure 2.4) and propagated as a periodic disturbance of the electromagnetic field when an electric charge oscillates or accelerates [2]. Due to the highly conducting nature of water, few underwater RF systems have been developed, even though these systems have been investigated since the very early days of radio, and had received considerable attention during the 1970s [2].

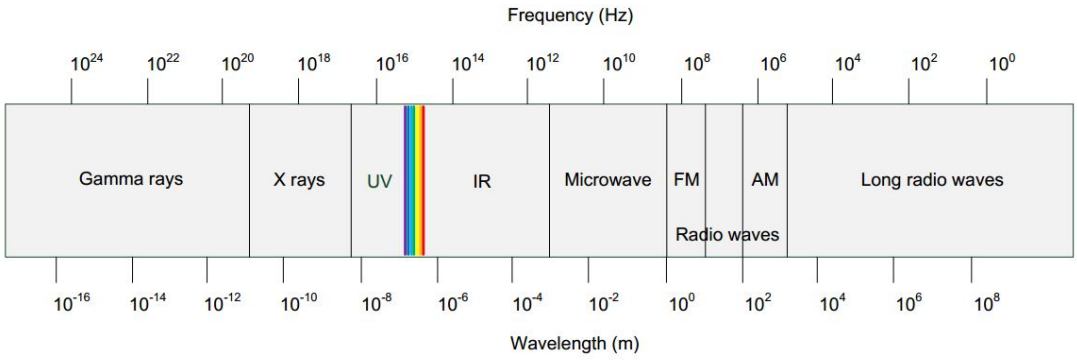

Figure 2.4: Electromagnetic Spectrum [2]

Unlike acoustic waves, EM waves can be used in shallow water. EM transmissions are tolerant to turbulence caused by tidal waves or human activities, as opposed to acoustic and optical waves, which are not [6]. They are unaffected by turbidity and pressure gradients and immune to acoustic noise [7]. In addition, they are unaffected by multi-path and effects on marine animals have not yet been detected [8]. Underwater communications based on EM waves are faster and can be used in higher working frequencies (which results in a higher bandwidth). However, they are susceptible to electromagnetic interferences (EMI) [7]. Their main problem is the high signal attenuation due to the conductivity of the water. This fact implies short communication distances between devices, so EM are never chosen for long distance communications. In Section 2.1.3.1, underwater propagation of RF waves is described.

Concerning RF-based underwater communication systems, the number of commercially available systems is reduced, mainly because of the lack in research and investment in this area where theoretical models show pessimistic scenarios. In fact there is not too much documentation about high frequency in underwater communications because most of the works are designed for low frequencies in order to achieve longest communication distances, preventing the strong attenuation generated in high frequencies. In RF communications, researchers work with Very Low Frequency (VLF), decreasing the frequency in order to have a more effective range of communication. For instance, in [9], they performed simulations at 3 kHz with distances between nodes of about 40 meters. In [10], the authors determined the maximum ranges for low frequencies, obtaining approximately 6 m at 100 kHz, 16 m at 10 kHz, and 22 m at 1 kHz.

When using high frequencies around 2.4 GHz, [7] evaluates RTT and packet loss on different frequencies and modulations, in function of the distance. Their results show the best case scenarios in 2,412 GHz, 2,437 GHz and 2,472 GHz frequencies. In the 2,412 GHz frequency, they achieve best results using 11 Mbit/s transfer rate (CCK modulation) with a maximum distance of approximately 15cm. In the 2.437 GHz frequency, their best result is using 1 Mbit/s transfer rate (BPSK modulation), also at a maximum distance of approximately 15cm. At 2.472 GHz frequency, the best case was with 11 Mbit/s transfer rate (CCK modulation), and again at a maximum distance of

15cm. Although, they conclude BPSK may be better compared to other modulations because this modulation uses only 2 symbols, so it has lower error probability.

As previously stated, commercial RF-based underwater systems are very scarce. WIRELESS FOR SUBSEA (WFS) sells some underwater solutions. The one offering the highest data rate has the name Seatooth® S300 [11], with 75 kbit/s to 156 kbit/s transfer rate and a maximum communication range of 6 meters, using an external 0.75m loop antenna, according to the data sheet. A picture of this device is shown in Figure 2.5.

As a conclusion, RF technology applied to underwater communications have the possibility to provide data rates never achieved by acoustic or optical systems. It has the disadvantage of allowing short ranges only, but the almost immunity to environmental characteristics makes it a good candidate for some scenarios. While most of research and investments are focused on the previous systems, we believe Wi-Fi based communications are the way to go, or at least should receive more attention, in order to supply short range applications the best solution possible in terms of speed, costs and reliability. This dissertation is about testing the viability of these systems.

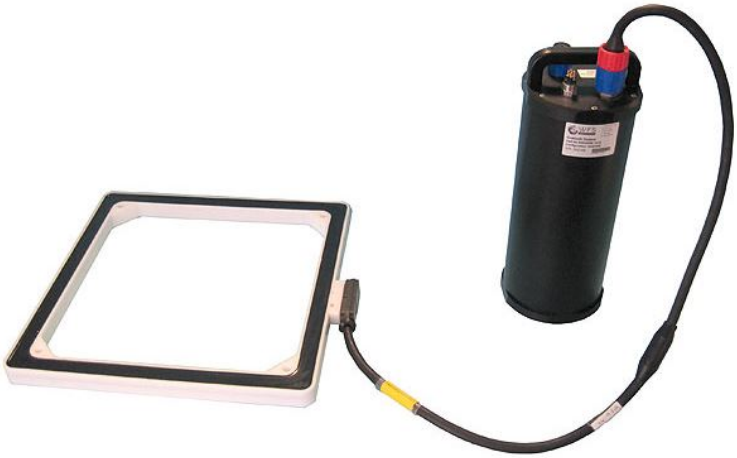

Figure 2.5: Seatooth® S300 Modem

2.1.3.1 Propagation Models

RF waves propagate slower in water than in the air. Because water contains dissolved salts and other matter, it becomes a partial conductor. The higher water's conductivity, the greater the attenuation of radio signals. While sea water has a high salt content, with an average conductivity of 4 Siemens/meter (S/m), fresh water conductivity is typically about 0.01 S/m [2].

According to [12], the propagation constant of water is given by Equation 2.1.

$$\gamma = \sqrt{j\omega\mu(\sigma + j\omega\varepsilon)} = \alpha + j\beta \ \left(\mathrm{m}^{-1}\right) \tag{2.1}$$

where σ is the conductivity of water in S/m, μ the permeability in N/A^2 and ε the permittivity in F/m. If the medium is not free space, the propagation constant γ is a complex quantity with α (the attenuation factor) and β (the phase factor) defined by Equation 2.2 and 2.3 [1].

$$\alpha = \omega\sqrt{\mu\varepsilon}\left[\frac{1}{2}\left(\sqrt{1+\left(\frac{\sigma}{\omega\varepsilon}\right)^2}-1\right)\right]^{\frac{1}{2}} \quad (\text{Np/m}) \tag{2.2}$$

$$\beta = \omega\sqrt{\mu\varepsilon}\left[\frac{1}{2}\left(\sqrt{1+\left(\frac{\sigma}{\omega\varepsilon}\right)^2}+1\right)\right]^{\frac{1}{2}} \quad (\text{rad/m}) \tag{2.3}$$

Permittivity $\bar{\varepsilon}_r$ is dependent of the complex frequency and commonly described with the Debye model as:

$$\bar{\varepsilon}_r = \varepsilon_\infty + \left[\frac{\varepsilon_s - \varepsilon_\infty}{1+\left(j\frac{f}{f_{ref}}\right)}\right] - \frac{j\sigma}{2\pi f\varepsilon_0} \tag{2.4}$$

where ε_s and ε_∞ are the real relative permittivity at low and high frequencies in F/m, respectively, f_{ref} is the relaxation frequency in Hz and ε_0 is the dielectric permittivity of free space in F/m. Wavelength λ and propagation speed v_p result in Equation 2.5 and 2.6.

$$\lambda = \frac{2\pi}{\alpha} \quad (\text{m}) \tag{2.5}$$

$$v_p = \frac{\omega}{\beta} \quad (\text{m/s}) \tag{2.6}$$

Received power as a function of transmitted signal, path loss and antenna gain at the receiver end can be described by Equation 2.7 [13].

$$P_{rec}(dBm) = P_t + G_t + G_r - L_{pathloss} \tag{2.7}$$

where P_t is the transmit power in dBm, G_r and G_t are the gains of the receiver and transmitter antenna in dBi and $L_{pathloss}$ is the path loss in water.

Free Space Path Loss is shown in Equation 2.8. This loss combined with attenuation in Equation 2.2 represent the total Path Loss attenuation referenced in Equation 2.7.

$$FSPL(dB) = 10log_{10}\left(\frac{4\pi}{c}df\right)^2 dB \tag{2.8}$$

From [14] and [15] an approximation model for underwater Propagation Loss can be described and is shown below:

$$L_{fresh\_water} = 0.0173\sqrt{f \times \sigma} \quad dB/m \tag{2.9}$$

Figure 2.6 plots Propagation Loss models from Equation 2.2 and Equation 2.9. We can see that both models follow similar values for frequencies lower than 1 MHz. From this point on, they show very different results. While 2.2 represents a complex model valid for all frequencies, we can conclude model 2.9 is only a good approximation for under 1 MHz.

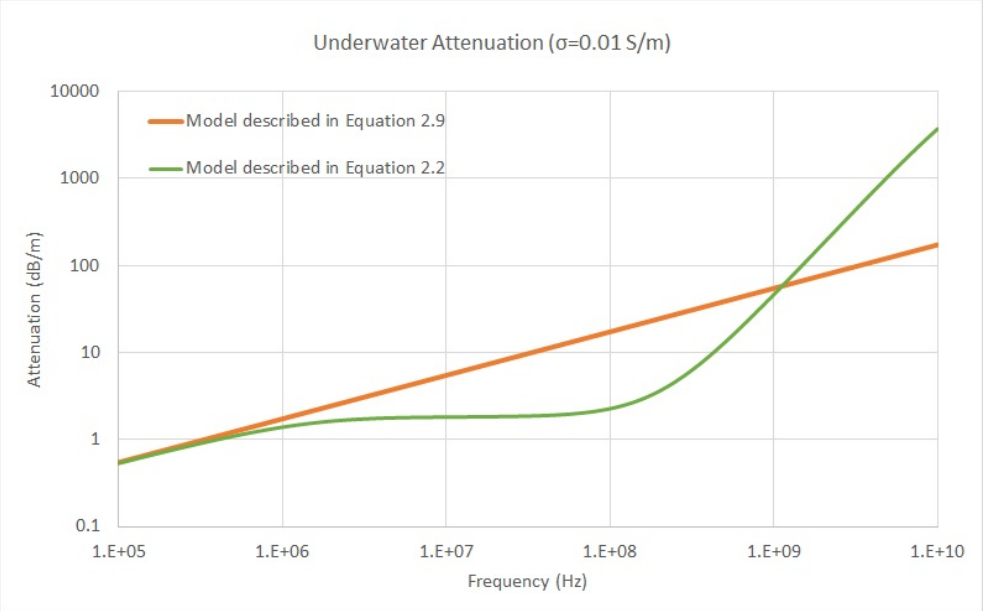

Figure 2.6: Comparison of propagation models.

2.2 IEEE 802.11

Although Wi-Fi is nowadays a term generally used for any wireless local area networks (WLANs) products, it is correctly applied to define products that are based on the IEEE 802.11 standards.

IEEE 802.11 is a set of media access control (MAC) and physical layer (PHY) specifications for implementing wireless local area network (WLAN) computer communication in the 2.4, 3.6,

5 and 60 GHz frequency bands. They are created and maintained by the IEEE LAN/MAN Standards Committee (IEEE 802). The base version of the standard was released in 1997 and has had subsequent amendments as shown in Table 2.3.

Table 2.3: IEEE 802.11 PHY STANDARDS

Release date	Standard	Band (GHz)	Bandwidth (MHz)	Modulation	Advanced antenna technologies	Maximum data rate
1997	802.11	2.4	20	DSSS,FHSS	N/A	2 Mbits/s
1999	802.11b	2.4	20	DSSS	N/A	11 Mbits/s
1999	802.11a	5	20	OFDM	N/A	54 Mbits/s
2003	802.11g	2.4	20	DSSS,OFDM	N/A	54 Mbits/s
2009	802.11n	2.4,5	20,40	OFDM	MIMO	600 Mbits/s
2012	802.11ad	60	2160	SC,OFDM	Beamforming	6.76 Gbit/s
2013	802.11ac	5	40,80,160	OFDM	MU-MIMO	6.93 Gbit/s

2.2.1 IEEE 802.11a/g/n standards

For this thesis in particular, the objective is to make use of globally used and distributed Wi-Fi equipments. We are using IEEE 802.11 a/g/n standards as these are the standards present in most Wi-Fi equipments. Devices running the latest IEEE 802.11ac standard are already in the market, but are not subject to this work, as are not widely diffused. IEEE 802.11 uses several modulation and coding schemes at the physical layer namely, DSSS, FHSS, OFDM and HR-DSSS.

2.2.1.1 IEEE 802.11a

IEEE 802.11a was the first approved extension to the 802.11 standard. It defines improvements and an additional modulation technique for transmitting data between stations. This extension adopts the Orthogonal Frequency Division Multiplexing (OFDM) scheme to the physical layer, which supports rates up to 54 Mbit/s operating in the Unlicensed National Information Infrastructure 5 GHz band. The OFDM modulation scheme in 802.11a is based on the principle of sub-carriers which are orthogonal to a base sub-carrier. Each subcarrier is modulated from a high-speed binary signal divided into several lower speed signals, in conjunction with one of the channels in the same band.

2.2.1.2 IEEE 802.11g

IEEE 802.11g extends the physical layer of 802.11 wireless local area networks with rates up to 54 Mbit/s using the same frequency 11 band as 802.11b. This extension is backwards compatible with the 802.11b extension and the two are commonly used together when deploying 802.11 wireless networks. The physical modulation scheme used in 802.11g networks is the same OFDM scheme as used in 802.11a. Data rates supported in 802.11g are 6, 9, 12, 18, 24, 36, 48 and 54

Mbit/s. The 802.11g standard falls back to CCK (used in 802.11b) for the 5.5 and 11 Mbit/s rates, and DBPSK/DQPSK+DSSS as used in the legacy 802.11 standard for 1 and 2 Mbit/s.

2.2.1.3 IEEE 802.11n

IEEE 802.11n is the fifth amendment for the 802.11 standard. This amendment provides, among several other things, the ability to use wider channels, frame aggregation and delayed acknowledgments. The physical layer of IEEE 802.11n can operate in three modes being: Non-HT (Legacy) Mode, HT Mixed Mode and High Throughput (Greenfield) Mode. These modes define compatibility options between 802.11 versions. 802.11n also improves the previous 802.11 standards by adding multiple-input multiple-output antennas (MIMO), so the data rates can be multiplied by the number of antennas to a max of 600 Mbit/s.

Chapter 3

Testbed Design and Optimization

In this chapter we describe the steps involved to build the testbed. These steps include the application of theoretical underwater propagation models, the selection of hardware and software used and study the optimization of antennas for the underwater scenario, aiming to achieve better performance results.

3.1 Propagation Models for 768 MHz, 2.462 GHz and 5.240 GHz

The objective of this dissertation is to evaluate the performance of Wi-Fi underwater communications at different frequencies used by widespread Wi-Fi devices. Currently, the most common standard is IEEE 802.11n which works at 2.4 GHz and 5 GHz band frequencies. Another possibility is to test the IEEE 802.11g standard using a 768 MHz carrier. This frequency, although a license is needed, became available after digital television was implemented. Unassigned or unused frequencies in the VHF and UHF television broadcast bands are called TV White Spaces. Since these frequencies are in the MHz order, this will allow a significantly increase in the communication link, meaning that greater distances are going to be achieved compared with the traditional 2.4 and 5 GHz Wi-Fi where the signals are absorbed more easily, in both the air and underwater medium. TV White Spaces frequencies are currently being explored for new Wi-Fi standards such as the recently approved IEEE 802.11af standard [16] [17].

Applying the propagation models, given in Section 2.1.3.1, to these frequencies result in Propagation Speeds and Attenuations shown in Table 3.1. The wavelength of a certain frequency is obtained dividing the propagation speed with the value of the frequency. Results presented in the table suggest that air adapted antennas, when submerged will become adapted to lower frequencies, resulting in a reduction on performance using the initial frequency. As will be described later in this section, our antennas will be implemented inside a waterproof case and thus electromagnetic waves will not only be in contact with water, but also air and the case material. Because of this, these propagation speed values will not be totally reflected in the performance results.

The water's conductivity value used was 0.01 S/m. As detailed in Section 4.1.1, the frequency used on the 700 MHz band was 768 MHz, one of the frequencies available of the wireless card

Ubiquity XtremeRange 7 [18] to operate with 20 MHz channels. Further details are presented in Section 3.2.4.3. The frequencies used in the 2.4 and 5 GHz bands were 2.462 and 5.240 GHz, respectively. More information regarding these frequencies can be seen in Section 3.3.2.1 and Section 3.3.2.2.

Table 3.1: Propagation Speed and Attenuation for 768 MHz, 2.462 GHz and 5.240 GHz frequencies in Fresh Water ($\sigma = 0.01$ S/m)

	Frequency		
	768MHz	2.462GHz	5.240GHz
Propagation Speed (m/s)	3.33×10^7	3.35×10^7	3.43×10^7
Attenuation (dB/m)	28	269	1161

For a wider view of underwater attenuation, Figure 3.1 shows a range of frequencies from 100 kHz to the 10 GHz frequency. Propagation models will help to acquire a previous notion of the possible experiences output.

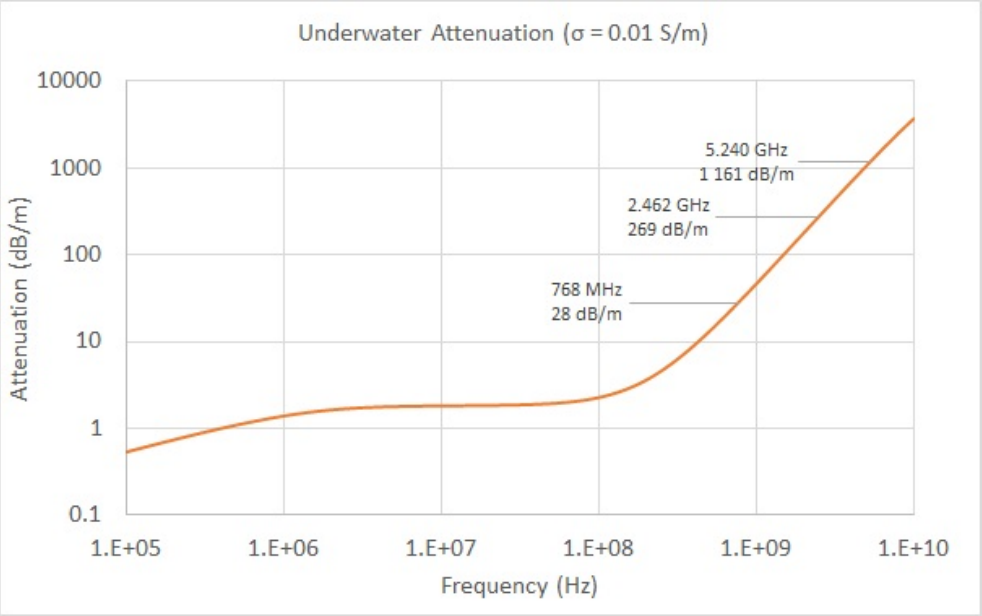

Figure 3.1: Propagation Loss vs Frequency

As presented in Figure 3.1, we can observe a strong increase of attenuation with the frequency. This represents a challenge when in underwater communications, because its high attenuation drastically reduce the maximum communications distance. Frequencies in the 770 MHz range may provide systems with longer distances when compared with 2.4 and 5 GHz bands. Apart from the 5 GHz band where the attenuation is very high, RF technology has the potential to provide high communication data rates but only at short ranges.

3.2 Underwater testbed

In this Section we present all the components of the testbed, including the environment where the experiences took place, the mechanic system to support them and the components of the underwater nodes. Every accessory was chosen with the criteria of this introducing a minimum or none undesired impact to the experiments.

3.2.1 Environment

The experiences took place in a Fresh Water tank placed in INESC TEC Robotics facilities [19]. Its dimensions are 10 meters long, 6 meters wide and 5 meters deep. Figure 3.2 tries to give a view of the tank.

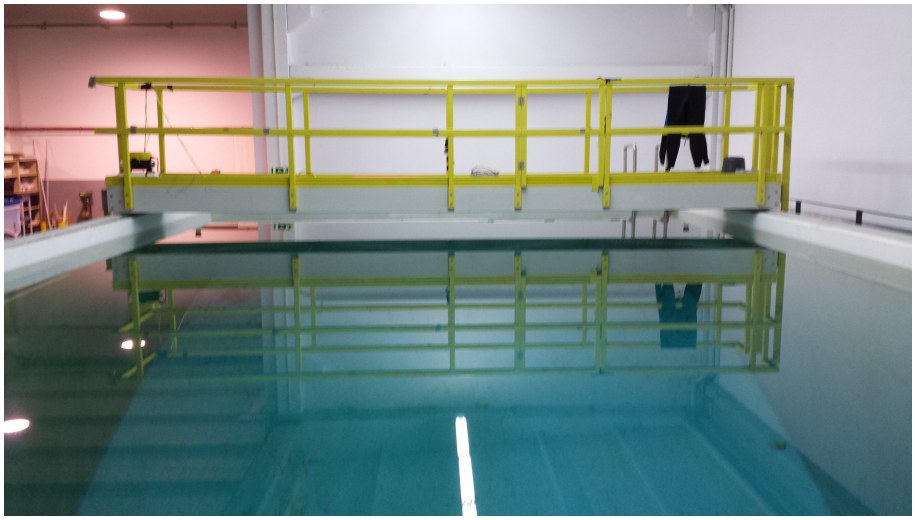

Figure 3.2: INESC TEC Robotics Fresh Water Tank

Since the 700 MHz band is subject of evaluation in this thesis, and being this frequency's theoretical distance higher than using 2.4 or 5 GHz, an underwater test between 2 nodes operating at this frequency was performed in order to have a reference of a possible communication range. This experiment showed that communication was possible with a distance of at least 140 cm. Taking this value into account it was important to ensure three situations:

- The distance between each 2 nodes was enough to reach the maximum potential distance of communication for that frequency.
- The distances from the nodes to the wall at the sides and behind them would be enough to avoid that the signal is propagated through the walls instead of through the water only.
- The depth of the tank was enough to ensure that no communication is made over-the-air. This requires that the sum of the depths of both nodes has to be higher than the direct underwater distance.

According to these requirements the tank was suitable for the experiences. The tank was filled with fresh water coming from a well, and a treatment with chlorine was periodically made. As shown in Section 2.1.3.1, the attenuation of electromagnetic waves underwater increases with the increase in its conductivity. Measurements to the temperature and conductivity of the water were made. In order to avoid using a water sample that would mislead results due to its particular depth and position, 3 samples from different locations were analyzed. The measurements were performed using an inoLab Cond Level 1 from WTW [20]. After calibrating the sensor with distiled water the results were:

- Temperature: $\approx \frac{T_{Sample1}+T_{Sample2}+T_{Sample3}}{Number\ of\ Samples} \approx \frac{23.7+22.1+21.8}{3}$ ºC ≈ 22.5 ºC
- Conductivity: $\approx \frac{\sigma_{Sample1}+\sigma_{Sample2}+\sigma_{Sample3}}{Number\ of\ Samples} \approx \frac{497+481+484}{3}$ µS/cm ≈ 487 µS/cm $= 0.0487$ S/m

These results indicate that the water conduction is higher than the value used to calculate water attenuation shown in Figure 3.1, coming from Equation 2.2. The value used was 0.01 S/m. Because of the dependency on water's conductivity in the previous equation, we feel the need to apply this new value, shown in Figure 3.3. To understand the effects of Sea Water in attenuation, a 4 S/m conductivity was also added to the figure. Table 3.2 gathers underwater attenuation using the different conductivities for 768 MHz, 2.462 GHz and 5.240 GHz frequencies in dB/m.

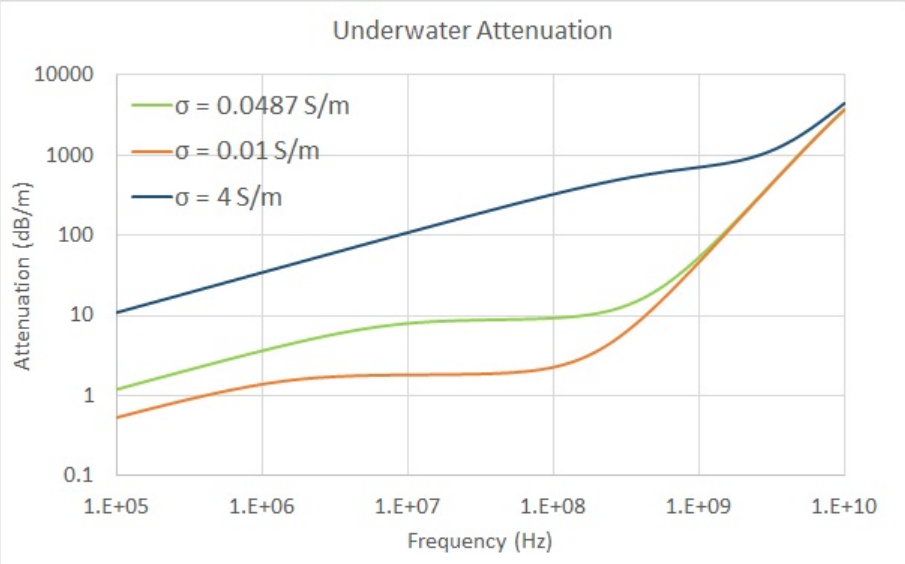

Figure 3.3: Underwater Attenuation using different conductivities.

Table 3.2: Attenuation for 768 MHz, 2.462 GHz and 5.240 GHz frequencies.

	Attenuation (dB/m)		
Conductivity (S/m)	**768 MHz**	**2.462 GHz**	**5.240 GHz**
0.01	28	269	1161
0.0487	35	278	1168
4	666	973	1880

As we can see from the Figure, not much higher attenuation values result when using a water conductivity of 0.0487 S/m. In fact, while values differ a maximum of 10 dB/m for frequencies under 1 GHz, above this point, very close attenuations are observed. In the 768 MHz frequency we now have 35 dB/m, 7 dB/m higher than using a conductivity of 0.01 S/m. In 2.462 and 5.240 GHz frequency, the model shows an attenuation of 278 dB/m and 1168 dB/m, respectively. It is important to say that this can be considered the worst case scenario for freshwater, since this value of conductivity is considered the limit for freshwater streams to support diverse aquatic life. Freshwater streams ideally should have a conductivity between 0.015 to 0.05 S/m. Typical conductivity for tap water in the city of Porto, where this dissertation was developed, reaches maximum values of 0.023 S/m. Regarding attenuation in Sea Water, this is much higher and will reduce drastically the range of underwater communications. A converging behavior can be seen for all the conductivities at distances close to 10 GHz.

3.2.2 System Overview

The testbed is composed of a total of 3 nodes for multiple access evaluation and a system to support and vary the distance of the nodes. The components are:

- **Clothes-line like System**: The need for having non-permanent, stable and easy to remove way of supporting the mobile node led to opting for this solution. This system also provides a fine control and tunning over the desired distance to establish between the nodes.
- **Underwater Nodes**: Each node includes a computer board, a Wi-Fi card, an antenna, a battery to supply power to the nodes that are not connected to the surface and weights to sink the node.
- **Surface Computer**: In order to start the evaluation processes an external computer was connected to one node.

A few possible solutions to support the nodes were considered but then discarded because it involved some risk of having electromagnetic waves being conducted through an indirect conductor other than the water. As said in the previous section, because of the theoretical distance of the 700 MHz band, this required the longer side of the water tank, with 10 meters long, to implement the clothes-line like system to support a mobile node. This was where the distance measures were made, using duct tape marks every 5 cm along the wire.

3.2.2.1 Point to Point

As first described in the Objectives of this dissertation, more precisely in Section 1.3, the First Phase is to evaluate a Point-to-point scenario. The node that would vary the distance was placed in the clothes-line system, while the other node was statically hanged in the bridge over the tank. Figure 3.4 represents a schema made before the actual material acquisition and implementation.

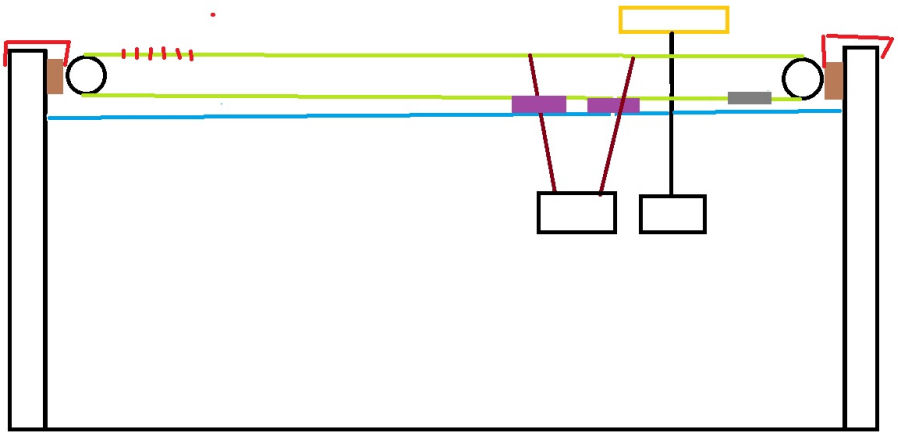

Figure 3.4: Clothes-line System Schema

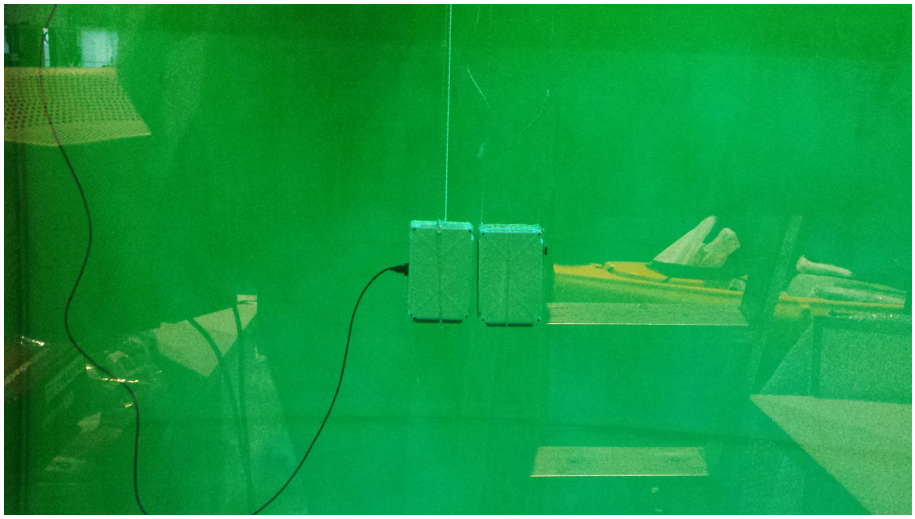

Figure 3.5: Nodes under the water.

As seen in Figure 3.5, one node was directly connected to the external computer, this cable also supplying power to the board. To avoid any propagation from one node to the other through the cable, we opted to totally isolate the second node, including, inside the waterproof case, a 12 V battery to power the system board. More details on the accessories used are found on Section 3.2.3.

3.2.2.2 3 Nodes: Multiple access

For this experiment the final decision was to place 2 nodes hanged from one side to the bridge and the other side to the clothes-line, while a 3rd node was in the clothes-line. This way, directionality could be easily given to the first 2 nodes. To properly evaluate multiple access, the 3 nodes were placed as an isosceles rectangle triangle as showed in Figure 3.6. Both the nodes hanged in

the bridge were power supplied with a battery to, like in the previous scenario, avoiding undesired propagation between the cables.

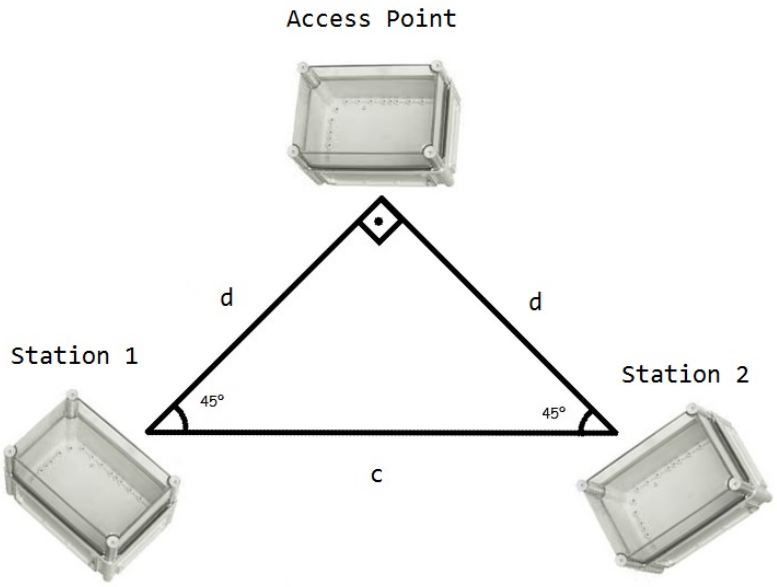

Figure 3.6: 3 Nodes Multiple Access Evaluation Scheme.

The way the nodes are positioned provide an easy setup to evaluate the performance of multiple access. While increasing the distance d in Figure 3.6, distance c will increase until a point where the stations can't hear each other while still being able to communicate with the Access Point. At this time, CSMA/CD (Carrier Sense Multiple Access Collision Detection) will not work properly and the Hidden Node Problem will occur. This situation causes multiple collisions at the Access Point, strongly reducing transmission quality. The objective of this experience is to detect at which distance this effect occurs and how it influences the transmission. Figure 3.7 present the implementation of this scenario at 2.4 GHz.

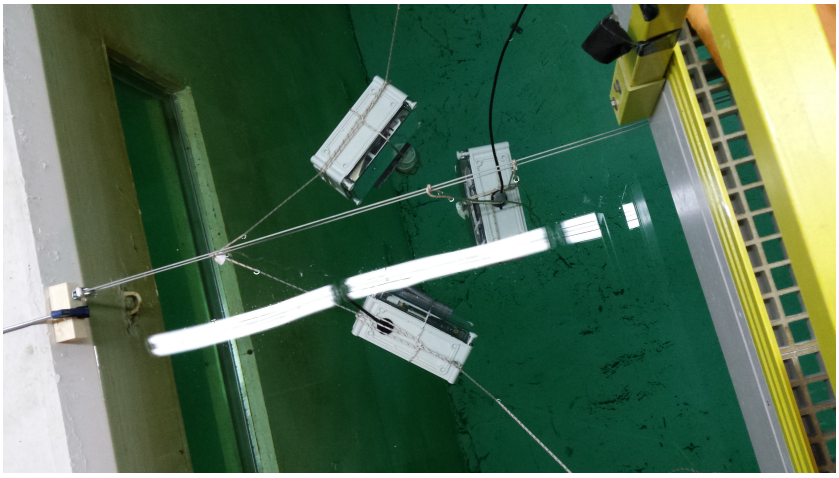

Figure 3.7: Implemented 3 Nodes Scenario.

3.2.3 Underwater Casing and Accessories

Before specifying the hardware and software in Section 3.2.4, this Section describes all the other system components, including the waterproof case, connectors, clothes-line composition and battery used.

- **Waterproof Case and Connectors:**

  The Waterproof case used for the experiences was the Fibox EKJVT 130 T [21] showed in Figure 3.8. It has a Polycarbonate material body, Ingress Protection classification of 67 (IP67) and dimensions of 280 x 190 x 130 mm. Being classified as IP 67, this indicates its protected against water immersion for 30 minutes at a depth of 1 meter, according to the IP code standard [22].

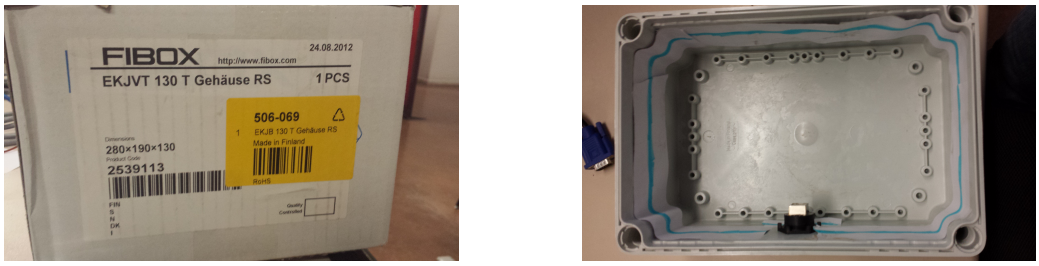

Figure 3.8: Fibox EKJVT 130 T Underwater Case.

In order to connect an external computer to an underwater node, a Bulgin PX0833 Cat5e IP68 rated connector was attached to the case. From this point to the computer, a Bulgin PX0836 cat5e 5 meters long cable was used, also having IP68 rating. When the connection was not needed a sealing cap maintained the waterproof protection. Both connectors can be seen in Figure 3.9.

(a) Bulgin PX0833 Cat5e.

(b) Bulgin PX0836 Cat5e.

Figure 3.9: Underwater Node Connectors.

Underwater theoretical results indicate the possibility of communication distances longer than 2 meters for the 770 MHz band frequency. That same distance should be used from the surface to the node, so any electromagnetic propagation over-the-air is avoided. Because the

rating of the case only guaranteed an immersion depth of 1 meter and for only 30 minutes, it was imperative to test if the case and connector were able to support at least a 2 meters submersion. The case was then submerged to 3 meters and was held underwater for at least 48 hours. When the case was extracted from the water, we observed no water inside, making the case suitable for the experiences.

- **Clothes-line like system**

The Clothes-line system had the goal to support the mobile node. For this system, the following components were acquired and put together: a pair of clamps, a pair of wood blocks, a pair of pulleys, a coated steel wire, a nylon cord and a tightener. Because we could not make any permanent changes to the environment, we had to use a clamp to fixate the wood block in the both sides of the water tank. The pulleys were then screwed in the wood block and the coated steel wire placed around these. The tightener was used to apply as much tension in the cord as possible so that the weight of the node would not force the wire down and influence the node's depth. Finally, a cord made of nylon was used, this to avoid any conductivity from the node to the steel wire, connected the case to the wire. This way, a stable and robust setup was implemented. Figure 3.10 shows the components used to build this clothes-line system.

(a) Clamp, wood block and pulley put together.

(b) Coated steel wire.

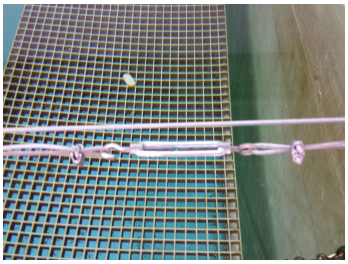

(c) Tightener to provide tension to the steel cord.

Figure 3.10: Components of Clothe-line system.

- **Battery**

To provide isolation to a node, the inclusion of a battery was needed. The battery used was a Haze HSC12-7, supplying 12 V and 7 A/h. Preliminary tests to the hardware setup indicated an average of 380 mA current consumption. The capacity of the battery could then power the hardware for a maximum of 17.5 hours. The battery has an approximate weight of 2 Kg.

Figure 3.11: 12V Battery used to supply the system boards.

- **Wheight Adjustment**

In order to know how much ballast the underwater node should have so it would sink, we had to look at the weights of the components and the dimensions and material density of the waterproof case. In short terms, an object will sink if its volume multiplied by its density can overcome the force of the water under it. The force of the water is the volume of the object multiplied by the water's density which is 1 g/cm^3. Using the dimensions of the case, we can say its volume is around 6900 cm^3. If all the content of the case was air, and because we can consider air density as being irrelevant for being so small (0.001225 g/cm^3), we would have to include inside the case a weight of 6900 g. Because we are using a battery inside, weighting around 2000 g, we would then only need 4900 g. The actual dimension of the case its constituted also by the case's material (Polycarbonate), which has a density of 1.21 g/cm^3. Although with little precision, we measured the inside of the case and got a volume of 5760 cm^3 of air, and the remaining 1156 cm^3 of Polycarbonate. Multiplying each volume by its density, the weight of the Polycarbonate is 1400 g and the weight of the air is 7 g, for a total of 1407 g. Finally, in order to know how much weight we need, we just subtracted to the water's weight (6900 g) the sum of the components inside which are: air and Polycarbonate (1407 g) , the weight of the battery (2000 g) and the weight of the system board (130 g). The value needed to sink the case is then 6900 - 3537 = 3363 g.

To apply this weight to the case, we used lead diving weights (Figure 3.12a) inside the case, and thin lead plates (figure 3.12b) coupled to the exterior of the case so we could future manipulate the case's stability.

(a) Diving Weights

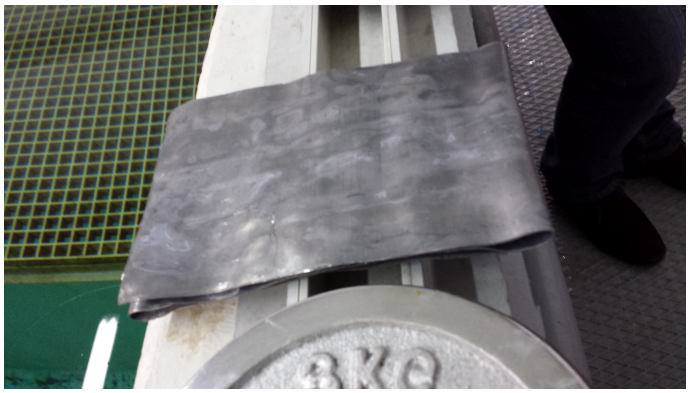

(b) Lead Plates

Figure 3.12: Underwater Node Sinking Weights.

3.2.4 Hardware Specifications

In this section all the Hardware components used are presented. We specify the computer board used and the wireless cards.

3.2.4.1 System Board PC Engines Alix3d3

The PC Engines ALIX3D3 is an Eurocard sized (100 x 160 mm) system board that allows a very large range of possible applications including wireless routers, firewalls or industrial user interface. Its 256 MB of DDR RAM and 500 MHz AMD Geode LX800 processor allows full range 32 bit x86 applications, while the architecture provides a good energy-efficient and compact solution. It can be powered using passive PoE on its LAN port, which was used in the experiments, providing power supply and communication with another device using the same RJ45 wire. The two Mini-PCI ports are used to accommodate the wireless cards that will be presented in the next section. The two USB ports were used either for inserting a keyboard or to load the Operating System. The robustness and viability of this device was proven in previous works made made at INESC TEC, removing any indecision about its use. More detailed and relevant specifications are shown in Table 3.3.

The compact size of this device is suitable for being enclosed in the waterproof case presented in Section 3.2.3.

Table 3.3: PC Engines Alix3d3 Specifications.

Parameter	Value
CPU	500 MHz AMD Geode LX800
DRAM	256 MB DDR DRAM
Power	DC jack or passive POE, min. 7V to max 20V
Expansion	2 miniPCI slots, LPC bus

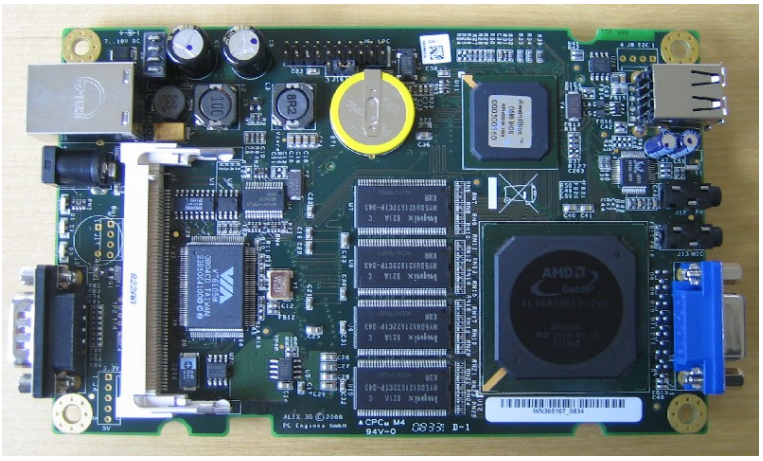

Figure 3.13: PC Engines ALIX3D3. [23]

3.2.4.2 RouterBOARD R52n-M: 2.4 GHz and 5 GHz bands

The miniPCI Routerboard r52n-M [24], shown in Figure 3.14, was the Wi-Fi module used. Its high performance in 802.11a/b/g/n standards, in both 2.4 and 5 GHz bands, provide a good communication solution. Sturdy MMCX connectors allows the use of any external antennas and adds extra durability. Supports 300 Mbit/s physical data rates and up to 200 Mbit/s of actual user throughput on both the uplink and downlink, using MIMO technology. Adding to this it can output up to 23dBm of transmission power. Using an Atheros AR9220 chipset, fully compatible drivers are available and extensively optimized for Linux operating systems, such as the ath9k driver. More relevant specifications of this wireless card are summarized in 3.4.

Table 3.4: RouterBOARD r52n-M Specifications. [24]

Card Parameter	Value
Chipset	Atheros AR9220
Standard	Dual band IEEE 802.11a/b/g/n standard
Output Power	up to 23 dBm
Antenna Connectors	Two MMCX Antenna Connectors
Operating temperatures	-50ºC to +60ºC
Performance	up to 300 Mbit/s physical data rates

Figure 3.14: RouterBoard r52n-M [24]

802.11n 2.4GHz	RX Sensitivity	Composite TX Power
MCS0 20MHz	-95	21
MCS0 40MHz	-90	21
MCS7 20MHz	-78	17
MCS7 40MHz	-75	16
802.11n 5GHz		
MCS0 20MHz	-95	21
MCS0 40MHz	-92	19
MCS7 20MHz	-77	16
MCS7 40MHz	-74	13

Figure 3.15: r52n-M RX sensibility and TX Power

Figure 3.15 shows the sensibility and TX power for different MCS (Modulation and Coding Scheme) and channel widths.

3.2.4.3 UBIQUITY XTREMERange7: 760-780MHz operating frequency

For the 700MHz band frequencies, the Ubiquity XTREMERange7 card was used (Figure 3.16). Using a down converter from 2.4 GHz, it provides operation in four channels between 760 and 780 MHz supporting 802.11b/g variants. Being a 32 bits miniPCI radio module it is fully compatible with the system board Alix3d3. Can also be set to operate with up to 20 MHz channel width in 2 of the 4 channel providing a maximum transmission data rate of 54 Mbit/s up to 28dBm of output power. Its Atheros chipset is also supported by stable Atheros family drivers for Linux, such as ath5k drivers. More technical specifications of the wireless card are summarized in Table 3.5.

Table 3.5: XTREMERange7 Specifications. [18]

Card Parameter	Value
Chipset	Atheros, 6th Generation, AR5414
Frequency Range	760-780 MHz
Interface	32-bit mini-PCI Type IIIA
Antenna Connectors	Two MMCX Antenna Connectors
Channel Bandwidth	5/10/20 MHz
TX Power	up to 28 +/- 1 dBm
Operating Temperatures	-45ºC to +90ºC

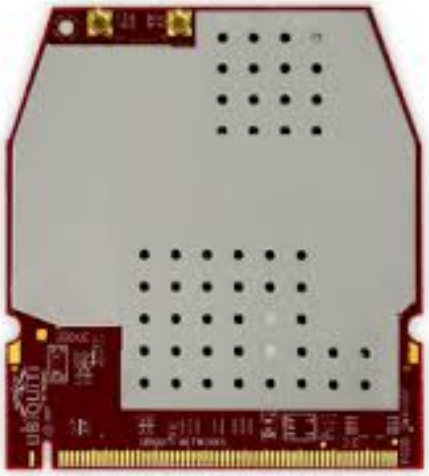

Figure 3.16: XtremeRange7 wireless card. [18]

The Sensitivity and TX Power, along with their tolerance, is present in Figure 3.17, for each modulation possible using IEEE 802.11g standard.

	DataRate	Sensitivity	Tolerance	TX Power	Tolerance
OFDM	6Mbps	-92 dBm	+/-1dB	28 dBm	+/-1dB
	9Mbps	-91 dBm	+/-1dB	28 dBm	+/-1dB
	12Mbps	-91 dBm	+/-1dB	28 dBm	+/-1dB
	18Mbps	-88 dBm	+/-1dB	28 dBm	+/-1dB
	24Mbps	-84 dBm	+/-1dB	28 dBm	+/-1dB
	36Mbps	-81 dBm	+/-1dB	26 dBm	+/-1dB
	48Mbps	-75 dBm	+/-1dB	25 dBm	+/-1dB
	54Mbps	-72 dBm	+/-1dB	24 dBm	+/-1dB

Figure 3.17: XR7 Sensibilities and TX Power using IEEE 802.11g Standard. [18]

3.2.5 Software

Even if the hardware presented in the previous section has the potential to provide a good setup for this thesis evaluations, without proper software to handle the devices, this can not be done. This Section refers to all the software, including operative system, wireless drivers and additional tools used, aiming to extract the full potential of the hardware and successfully retrieve reliable data of the experiments.

3.2.5.1 Operating System and Wireless Drivers

The starting point for the operating system was to use OpenWRT Linux based operating system. OpenWRT is a free and open-source Linux distribution targeting embedded devices. It is mostly used in router boards providing full customization of the wireless cards using its HTTP user interface or SSH access. The images of OpenWRT versions were downloaded already compiled directly from the official OpenWrt download website [25].

Preliminary tests showed that kernel version r36088 (also known as Aptitude Adjustment 12.09) together with the driver ath9k 3.3.8+2012-09-07-3, worked as intended with the r52n-M wireless card for the 2.4 and 5 GHz bands. As for the 700 MHz band wireless card, when testing the ath5k driver version 3.3.8+2012-09-07-3, we witnessed some strange behaviors when testing the throughput, including kernel panics and the TX power would not change according to the value set. It was then decided to test the trunk OpenWRT kernel version coming along with version 3.10.36+2014-05-22-1 of the ath5k driver. In this case, with the help of measurements using a Spectrum Analyzer, the communication became stable and the TX power change correctly.

3.2.5.2 Additional Software

Additional tools were required to proceed with the performance measurements. These tools come in the form of packages, installed directly over the operative system OpenWRT:

- **Iperf** is a traffic generator software used to measure network performance. It allows to create UDP/TCP data streams in order to measure throughput, delay jitter, and packets loss.
- **Iwinfo** is a tool to monitor a set of parameters of the wireless card, including Output Power, Signal and Link Synchronized Throughput.

To easily retrieve the relevant parameters from within the logs generated by the tool Iperf, an awk[1] script was made and results were treated using Microsoft Office Excel.

3.3 Antennas: Analysis and Adaptation

Because of the lower propagation speed of electromagnetic waves underwater when compared to air, the wavelength for a given frequency is lower too. This means that an antenna designed

[1] AWK - interpreted programming language designed for text processing.

to work at a certain frequency over-the-air, when submerged, will be adapted, not to work in the same frequency, but at a lower value. This fact caused the need to test these antennas using a Network Analyzer and measure the s11 parameter, which provides the return loss in dB. With this we could see and validate the change in the frequency. Also, since the underwater nodes include a lead battery right next to the antennas, we knew previously that this would affect the frequency and/or the percentage of irradiated energy. This required that tests to the antennas would be made with the antenna inside the node with the components included.

In order to better understand the next results, Equation 3.1 [26] represents the conversion of the Return Loss (dB) to Match Efficiency (%). RL stands for Return Loss.

$$Efficiency = 100 \times \left(1 - \left(\frac{-|RL|}{10}\right)^{10}\right) \quad (\%) \tag{3.1}$$

Computing some relevant values of Return Loss into Match Efficiency in Table 3.6, we can see that a Return Loss of 10 dB or higher will result in an efficiency of at least 90%.

Table 3.6: Conversion between Return Loss and Match Efficiency.

Return Loss (dB)	4	5	6	7	8	9	10	11	12	13	14	15	16
Match Efficiency (%)	60	68	75	80	84	87	90	92	94	95	96	97	98

This means that 90% of the transmission power will be successfully irradiated. Because of the presence of the lead battery, this might not be totally true since the battery may absorb some energy, leading to the possibility of an optimistic result. The Network Analyzer injects energy through the antenna and compares it to the energy reflected. If no energy is reflected it means that all the energy transmitted has propagated effectively out of the antenna, and likely out of the underwater node.

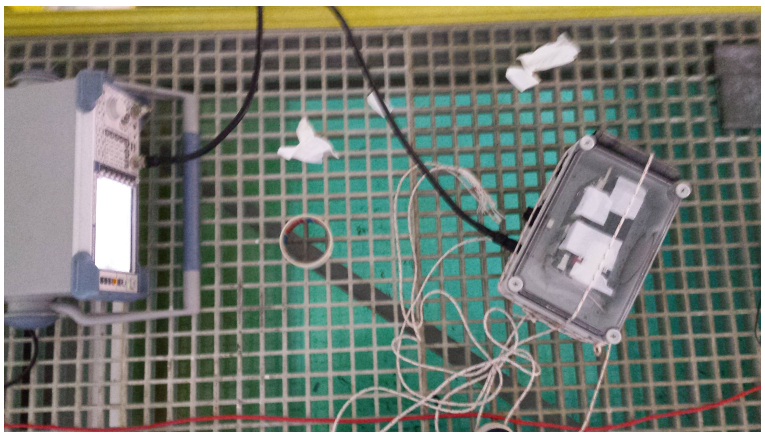

Figure 3.18: Rohde&Schwarz ZVL3 Vector Network Analyzer connected to the underwater node.

As seen if Figure 3.18, the Rohde&Schwarz ZVL3 Vector Network Analyzer had a LLC 400 cable connected to a type N connector attached to the waterproof case. This end of the cable

was covered with thermal sleeve to avoid the water to be in contact with the ground cable. All the components that would go inside the case when measuring performance parameters were included. The node was then submerged until a depth of at least 1m and the results were saved as dB/magnitude data and computed using Matlab.

Regarding the depth of the nodes, different measures showed that depths near the surface change the s11 parameter of the antenna, explained by the contact of the electromagnetic waves with the air at the surface. For various lower depths the s11 did not vary.

3.3.1 700 MHz Band Antenna

The antenna used for the 768 MHz test was a loop antenna. This antenna was created previously for a dissertation regarding open sea using the same wireless card [27]. It is an antenna easy to build, requiring just a copper cable with an acceptable width. Also, it is easy to cut and solder to the connector, if little adjustments are required.

Figure 3.19 shows the s11 parameter measurements from the Network Analyzer using the 768 MHz loop antenna above water outside and inside the case, and underwater.

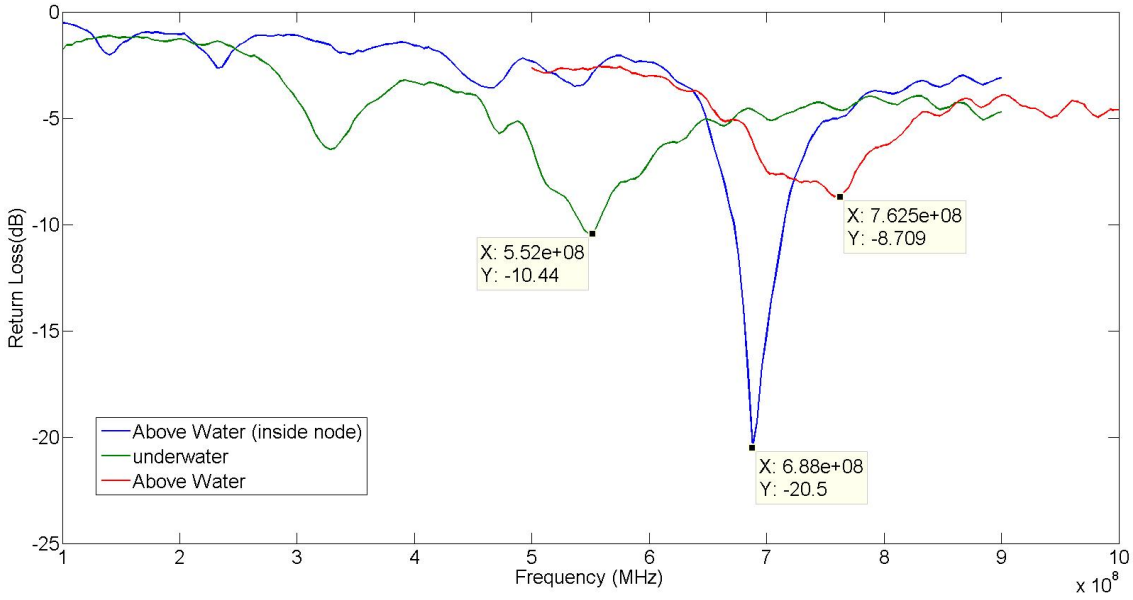

Figure 3.19: S11 values for the air adapted 768 MHz loop antenna.

As can be seen, the antenna's s11 parameter, measured outside the node above water, had its maximum return loss point around the 760 MHz frequency. This tells that this antenna was designed for air communications in the 750-770 MHz band frequency. When testing the antenna inside the node, but still outside the water, the case and the components caused a shift of the maximum point to the 690 MHz. When submerged we observed another shift of the maximum return loss point to the 550 MHz band frequency with s11 values around -10.5 dB. More important than

this, is the s11 value at 768 MHz. This is the frequency we will be using when testing underwater performance and the value of the s11 is less than -5 dB, meaning less than 68% non reflected energy transmitted. The wireless card XtremeRange 7, allows the use of a channel bandwidth of 20 MHz using the 768 MHz frequency, so observing return loss for a 20 MHz channel centered at 768 MHz, we obtain even worst values.

In order to reach a higher s11 value for the 770 MHz band when used underwater, an iterative process was made. Because we wanted to shift s11 to a higher frequency, we had to shorten the antenna size, to reflect a smaller wavelength. Starting with 3 mm cuts in the antenna length, we measured the s11 parameter for each iteration. After making some small 1 mm cuts, we reached an acceptable s11 value for the 768MHz frequency. Figure 3.20 shows measures to the old antenna (designed for air 770 MHz communications) versus the measures of the new adapted antennas. Because the 2 nodes had the batteries with different distances to the antennas, there was the need to make the iterative process for each node.

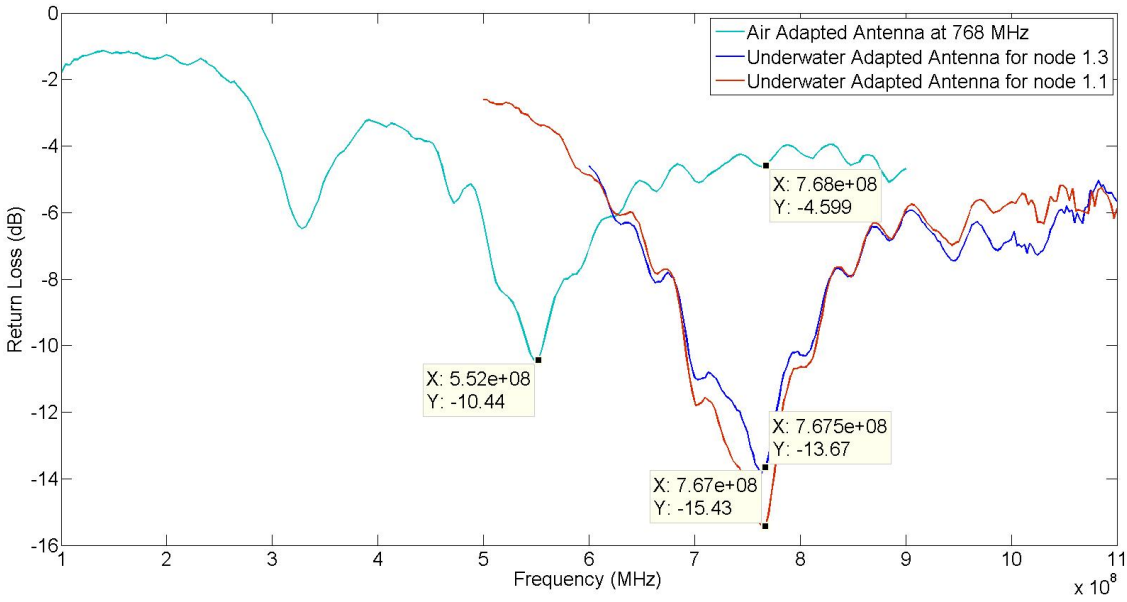

Figure 3.20: S11 values for the air-adapted 768 MHz and both water-adapted 768 MHz loop antennas.

Comparing the results shown in the above figure, we can see a lot better results using the new antennas for the center frequency of 768 MHz. At this frequency, the new antennas achieved a minimum return loss at 768 MHz of -13.60 dB and -15.40 dB. Considering the channel bandwidth of 20 MHz centered at 768 MHz, we can see a minimum of around -12 dB. This means a minimum of 94% energy is efficiently being irradiated from the antenna and thus producing better results from the previous antenna, which was less than 68%.

Figure 3.21: Air Adapted and Underwater Adapted (smaller) 768 MHz antennas.

The results were promising, because the efficiency of the transmission power improved from less than 68% to above 94%. Figure 3.21 shows the size difference between the air and water adapted antennas. The perimeter was measured which resulted in 0.3974 meters for the air adapted antenna and 0.3134 meters for the water adapted one.

3.3.2 2.4GHz and 5GHz Bands Antennas

For the 2.4GHz and 5GHz communications we used patch antennas with 9dBi gain for 2.4GHz, and 15dBi for the 5 GHz one. These antennas come inside StationBoxMikro [28] enclosure, from RF Elements. Since we only wanted the antennas, these were removed from the enclosure and positioned inside the case. They were chosen thanks to its high gain and reduced size, compatible with the waterproof case dimensions. Because omni directional antennas are the ones used in most of the Wi-Fi equipment, these were also submitted to these tests just to be recorded. Omni directional antennas are characterized by a wider angle of radiation but with a lower maximum gain comparing to the patches. In Figure 3.22 we show the radiation pattern of both the 2.4 and 5 GHz antenna patches, supplied by the manufacturer.

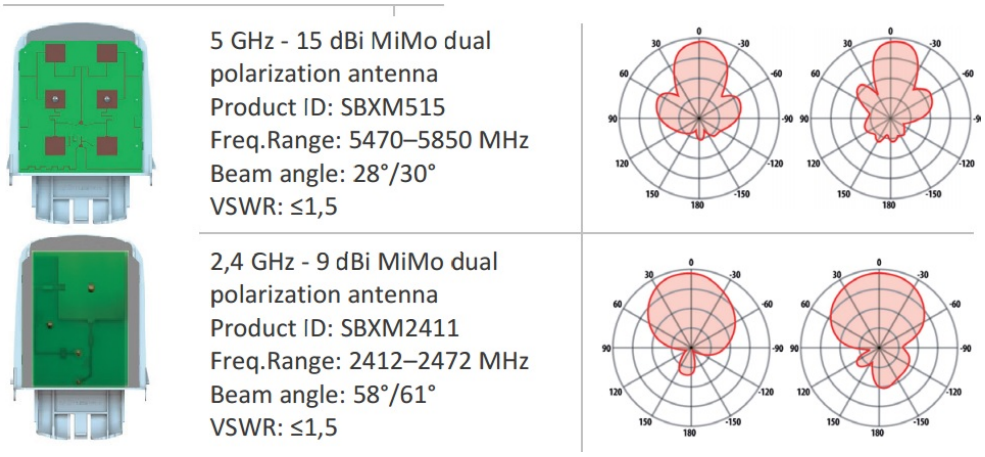

Figure 3.22: Radiation Pattern of 2.4 and 5 GHz patches [28].

3.3.2.1 2.4 GHz Patch

Figure 3.22 shows the results of the s11 parameter using the 2.4 GHz patch both outside the water (but still inside the node), and inside the water.

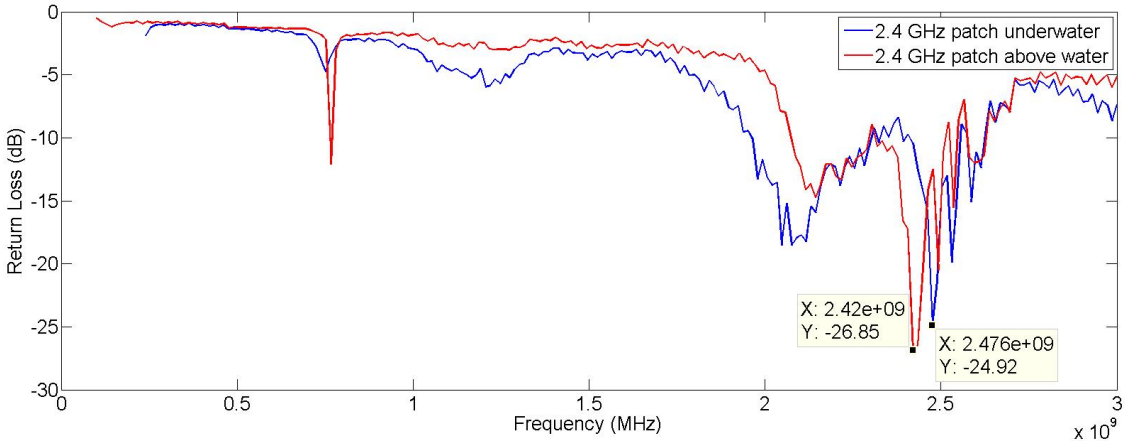

Figure 3.23: S11 for the 2.4 GHz Patch Antenna.

Using the 2.4 GHz patch antenna we observed a left shift in frequencies below 2.2 GHz, and showed the inverse behavior past that frequency. According to the figure, the best s11 parameter value underwater is observed on frequency 2.476 GHz. As it is indicated later in Section 4.1.2, the closest frequency able to be used with the wireless card is 2.462 GHz (channel 11). This frequency shows a return loss of -15.83 dB. Since the channel bandwidth used is 40 MHz, it is important to assure a good s11 value for all the 40 MHz channel. The transmission will use 20 MHz centered in 2.462 GHz and 20 MHz centered in channel 6 (2.437 GHz). The worst value of return loss for the 40 MHz bandwidth channel is at frequency 2.427 GHz with a value of around -12 dB. These are acceptable values since they correspond to a minimum of 94% efficiency according to Table 3.6.

Figure 3.24 plots the value of the s11 parameter using the omni directional antennas.

A similar left shift behavior was detected using omni directional antennas, but even more irregular than using the patch one. While showing good performance between the 2.4 and 2.58 GHz frequencies above water, the better return loss point was shifted to the 2.232 GHz frequency and poor performance was observed in the 2.4 GHz band, when tested underwater. Since our available highest frequency to work with the 2.4 GHz band is 2.462 GHz, when looking at the performance of this frequency we see values under -12 dB and similar ones for a 40 MHz channel bandwidth. These results point to the conclusion that the patch antennas are better to work underwater, in our particular setup.

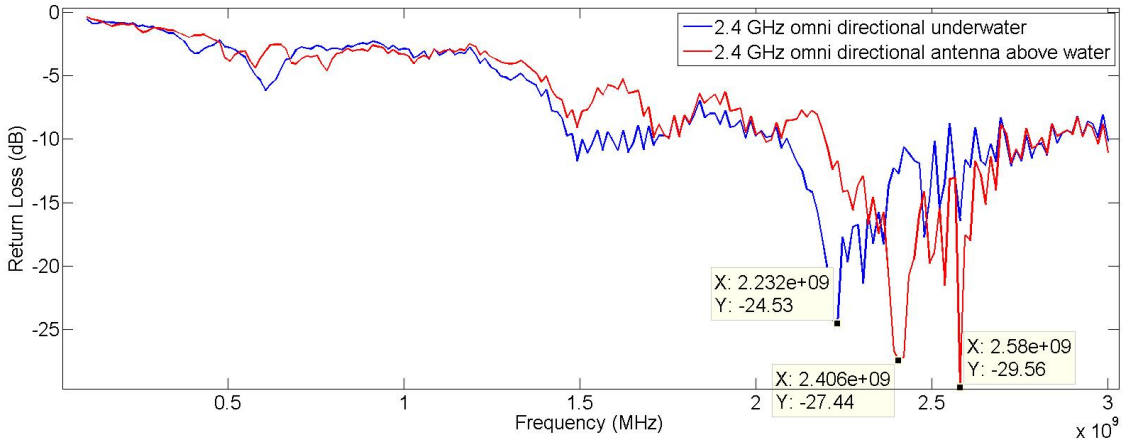

Figure 3.24: S11 for 2.4 GHz Omni Directional Antenna.

3.3.2.2 5 GHz Patch

Figure 3.25 shows s11 results for the 5 GHz patch antenna. The behavior observed is somehow related to the one seen using the 2.4 GHz patch antenna. We can see a small left shift until around 5.4 GHz, when the node is submerged, but a slightly right shift after this frequency.

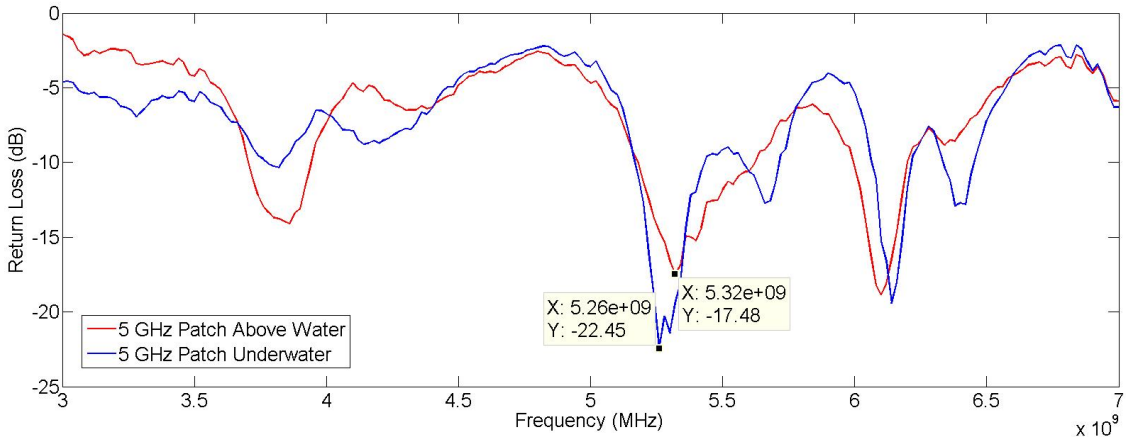

Figure 3.25: S11 for the 5 GHz Patch Antenna.

The frequency that shows the better match efficiency is frequency 5.26 GHz. The closest frequency able to use with the wireless card is frequency 5.24 GHz corresponding to channel 48. This point has a return loss of -19 dB, while the 40 MHz channel has a minimum of -13 dB at 5.21 GHz and a maximum of more than -20 dB at 5.25 GHz. The use of this channel provides a match efficiency of at least 95% and was used to achieve the results obtained in Section 4.1.3.

3.4 Conclusions

In this section we discuss the results from an overall perspective and draw the major conclusions.

A previous analysis to the antennas behavior underwater helped to understand that different types of antennas may experience different changes when submerged, but a left shift effect in frequency for the s11 values was common to all antennas. This is expected due to the lower propagation speed of electromagnetic waves underwater.

When using the 768 MHz frequency an adaptation was made reducing iteratively the length of the air adapted loop antenna, until acceptable values of s11 were observed at the desired frequency (768 MHz). The result was an improvement in that frequency from around -4 dB using the air adapted antenna, to a minimum of -12 dB using the underwater adapted antenna, considering a 20 MHz bandwidth channel. Converting s11 values to match efficiency, an improvement of almost 34% was achieved with the adaptation. This may lead to accomplish more stable communications and longer maximum distances between nodes.

When it comes to 2.4 and 5 GHz bands, the antennas used were patch antennas. Results show that a left shift in frequency was also present, when submerging the antenna, but until a certain point. From this point on the behavior inverted and a right shift was experienced. In the case of the 2.4 GHz antenna, the highest s11 value observed at the 2.42 GHz above water right shifted to the 2.476 GHz frequency underwater. Since it was possible to evaluate 2.4 GHz performance using a channel very close to this frequency, we opted not to make any changes. The 5 GHz patch showed similar results but this time a frequency where a left shift occurred was used. Above water a good s11 value was present at 5.32 GHz. When submerge,d this point left shifted to 5.26 GHz. Again, this frequency was able to use at the performance evaluation, so no changes to this antenna were made also. Omni directional antennas were analyzed but s11 values showed that this antenna would perform worse than the patch one, since when submerged, return loss for the 2.4 GHz band was lower.

Similar antenna analysis and adaptation in the 700 MHz band was not seen in other publications so far. In [29], an adaptation to sea water at 2.4 GHz is made achieving good s11 results, but no performance experiments were followed. Regarding the 5 GHz band, no related work was found.

Chapter 4

Performance Evaluation

In this chapter we present and analyze the results obtained from the experiments. We measured TCP and UDP throughput, delay jitter, Round Trip Time and RSSI, using 700 MHz , 2.4 GHz and 5 GHz frequency bands. We also make a comparison of the results obtained with the designed 768 MHz underwater loop antenna. A Point-to-Point scenario is evaluated for each frequency band, and a 3 nodes setup is tested in the 2.4 GHz frequency in order to test Multiple Access performance.

4.1 Point-to-Point

This section concerns the experiments using a Point-to-Point setup. As seen in Figure 4.1, both nodes were submerged to a depth of approximately 2 meters. While one of the nodes was totally isolated, the other was connected to an external computer. This cable had the purpose of supplying power to the board and providing a communication link to the board for configurations and information retrieval.

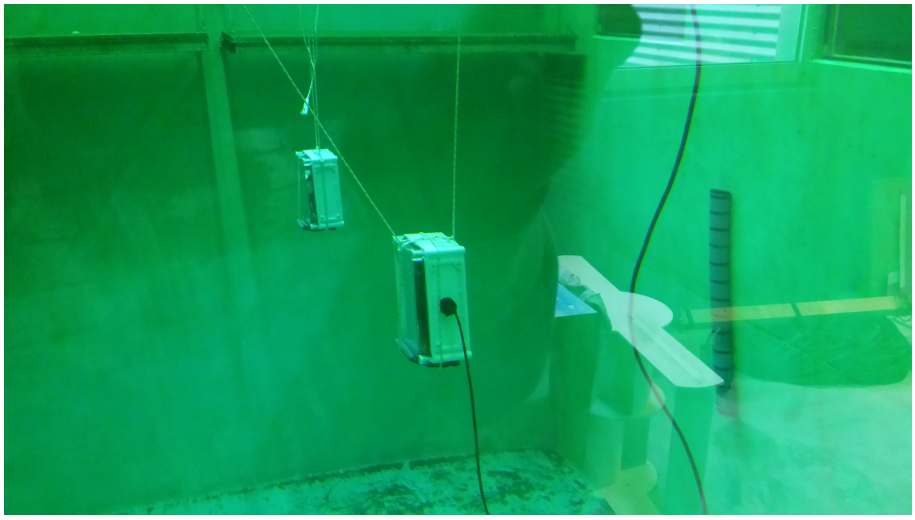

Figure 4.1: Point-to-Point underwater view.

The topology configured was an Ad-Hoc network with no security enabled. Static IP addresses were given to each node's wireless interface, in the 192.168.2.X range, while the Ethernet interfaces had IP addresses to be able to communicate with the external computer, within the 192.168.1.X range.

As shown in Figure 4.2, to measure the distance between the nodes, a 3 meter scale with intervals of 5 cm was represented in the clothes-line cord, using duct tape. Before each set of experiments, the cord was positioned in the first duct tape mark, and then the mobile node was placed in the desired initial position. After running the tests in a specific distance, the cord was pulled until the next desired mark, moving the node further from the static node.

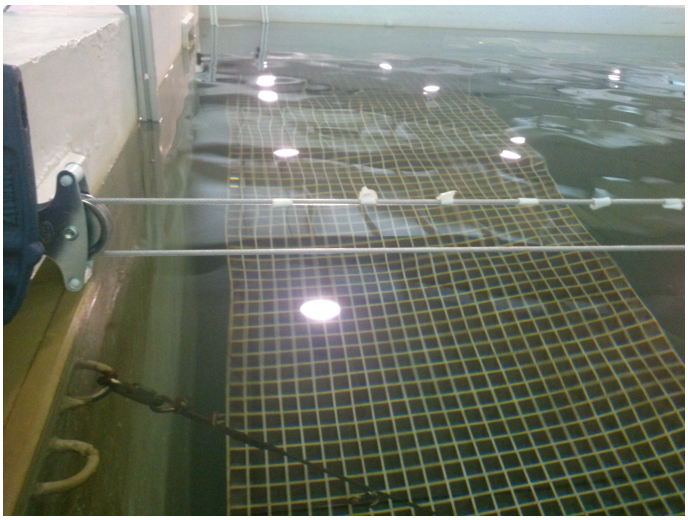

Figure 4.2: Clothes-line scale.

The commands to run the tools used to measure the communication parameters were inserted in a shell script running in one of the nodes. The script consisted on a for loop that ran 10 times for each distance. TCP/UDP Throughput and Jitter were measured using the tool Iperf. For every distance, 10 samples of 20 seconds each were acquired, these in intervals of 1 second. The average of each sample was then used to calculate the average of all the samples. Jitter and Lost Packets are parameters retrieved from the Iperf UDP connection. Iperf commands were configured to test bidirectional performance so the results reflect both directions of the link. Round Trip Time was measured using a ping command of 20 seconds for each iteration of the for loop. Finally, Iwinfo tool supplied each distance's RSSI, one sample recorded in each loop iteration. These values of RSSI were compared to the theoretical signal received provided by the Propagation Models in Section 2.1.3.1. The gains of the antennas and transmission power, as the losses caused by the cables and connectors, were taken into account when calculating the theoretical RSSI.

In order to provide better detail on each parameter's performance, a confidence interval of 95% was calculated for each parameter and applied to the average.

4.1.1 768 MHz Performance Results

This section addresses results using the 768 MHz frequency with both air and water adapted antennas.

Figure 4.3 represents the details on the down conversion of the 4 channels available to use with the wireless card XtremeRange7. It provides the carrier frequency and channel bandwidth. For our experiments we wanted the highest maximum throughput possible so it was used a channel able to use a 20 MHz bandwidth. Since there are 2 options (channel 5 or 6), we chose channel 5, with a carrier frequency of 768 MHz.

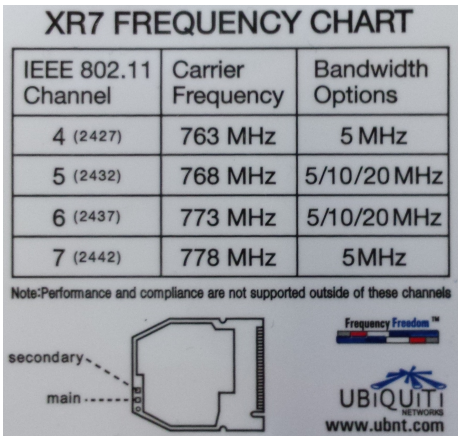

Figure 4.3: XR7 Frequency Chart

The transmit power was set to the maximum supported by the wireless card (28dBm). A summarization of all the configuration parameters is shown if Table 4.1. Parameters not represented were set to default.

Table 4.1: Summarization of Link Configurations. [18]

Link parameter	Value
Wireless Standard	802.11b/g
Network Mode	Ad-Hoc
Channel	5(2.432 GHz converted to 768 MHz)
Channel Bandwidth	20 MHz
TX Power	28 dBm
Bit rate	Auto
Noise level	-66 dBm
Pigtails and connectors Loss	< 2 dB
Loop Antenna Gain	< 2 dBi

4.1.1.1 No adaptation

In this Section we analyze the results obtained using the loop antenna designed to perform well over-the-air at frequencies in the 770 MHz band. Furthermore, a comparison between these

and the theoretical models provided in Section 2.1.3.1 is made.

- **Measured and Theoretical RSSI**

  Figure 4.4 shows RSSI measured and theoretical values. Regarding our experiences, for distances under 40 cm we can observe values higher than -20 dBm and sometimes reaching values higher than 0 dBm. Such high signals may be responsible of causing an amplifier compression at the receiver. As in over-the-air scenarios at this frequency such received powers are not likely to occur - 770 MHz links are designed for long range links. As the input level is increased beyond the linear range of the amplifier, gain compression will occur. This can cause many problems in the operation of the radio device such as inter-modulation distortion, cross modulation and blocking, limiting the potential of the link parameters. From that distance, RSSI values decay over the distance having an average of -55 dBm in the link limit (145 cm).

  Although results reported by the wireless driver suggest a sensibility around -66 dBm because of the minimum signal received, we believe these values are wrong and should in reality represent the wireless card sensibility presented in Figure 3.17, which is around -90 dBm, representing a 24 dB difference. Saying this, in order to properly compare results with the theoretical models, an offset of -24 dBm was made to the results experienced.

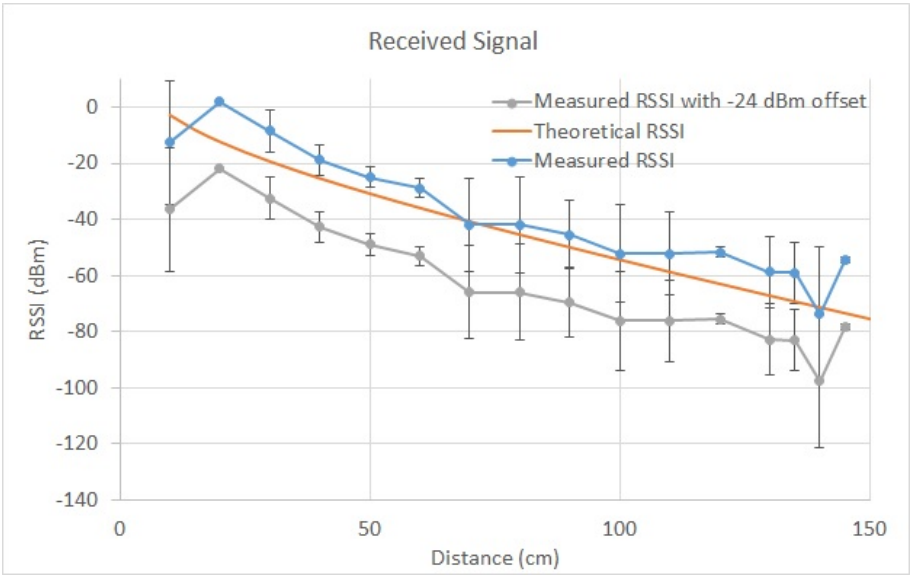

Figure 4.4: Measured vs Theoretical RSSI.

Comparing experimental results, with a -24 dBm offset, and theoretical results, we can see an overall difference of 20 dB. This difference may be explained by the antenna not being adapted to work at the specified frequency, resulting in a less efficient power transmission and thus, reducing the received signal.

- **TCP and UDP Throughput**

  Figures 4.5 and 4.6 present the TCP and UDP throughputs, respectively, for each distance.

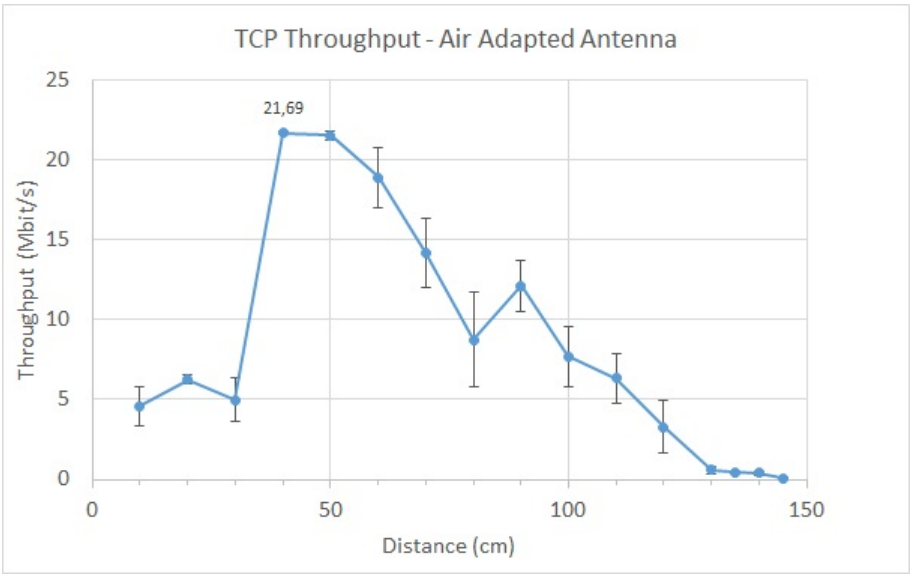

Figure 4.5: TCP Throughput

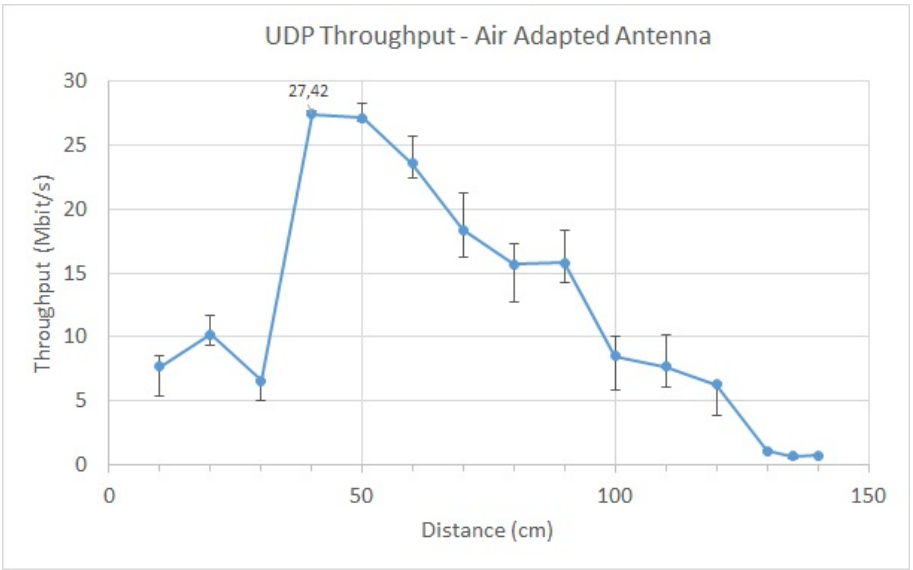

Figure 4.6: UDP Throughput

Looking at the TCP Throughput output in Figure 4.5 we can start by noticing the low values (around 5 Mbit/s) for distances lower than 40 cm. If we take a look at the RSSI values in Figure 4.4, we can see this is a zone where the signal reaches values close to or higher than 0 dBm. As pointed out in the RSSI measures section, this could be caused by an excess of signal at the receiver. This reduction in throughput was also observed in over-the-air

scenarios due to the same reason. These low values could be also explained if we were in the near-field zone. The near-field, which is the region between the antenna and the far field, is a region in which there are strong inductive and capacitive effects from the currents and charges in the antenna that cause electromagnetic components to behave differently, since these are oriented for far-field communications. The Far-field, or Fraunhofer region, of a transmitting antenna, is defined as the region beyond the far-field distance $d_f = \frac{2D^2}{\lambda}$, where D is the diameter of the antenna and λ the carrier wavelength [30]). Considering the underwater propagation speed obtained in Table 3.1, the resulting wavelength at 768 MHz is 4.34 cm. The diameter of our air-adapted antenna is about 12 cm, thus near-field effects could be experienced until a distance of around 66 cm, which is close to the distance until where we experienced low throughput values.

Around the 40 cm distance, this effect is no longer present, and a normal behaviour is observed. At 40 cm, an average of approximately 22 Mbit/s is achieved. This is a normal maximum value for TCP throughput using 802.11g standard and 54 Mbit/s bit rate. After 50 cm distance, the throughput starts to decay until reaching a minimum of around 50 kbit/s at 145 cm, being this the maximum distance of communication achieved with this setup. At 80 cm we can also see a slight throughput peak, possibly being caused by a change in the modulation, where this may be better synchronized with the link conditions.

Figure 4.6 represents the UDP throughput results. Analysing the graphic we can see a similar result to the TCP throughput, and thus, can use the previous description for the distance and throughput relation. The only difference is that with UDP packets, we can achieve slightly better throughputs for each distance. This is explained by UDP having less overhead and TCP ACKs not being accounted as throughput.

The maximum throughput achieved with TCP was around 22 Mbit/s, while with UDP, approximately 28 Mbit/s were reached. At the maximum distance of 140 cm, an UDP throughput of around 800 kbit/s was experienced.

- **Jitter and Round Trip Time**

Figure 4.7 refers to the Jitter using Iperf. We can see that jitter remains stable and lower than 10 ms until the distance reaches 110 cm. After this mark, jitter becomes more unstable and values around 50 ms were experienced until the maximum distance.

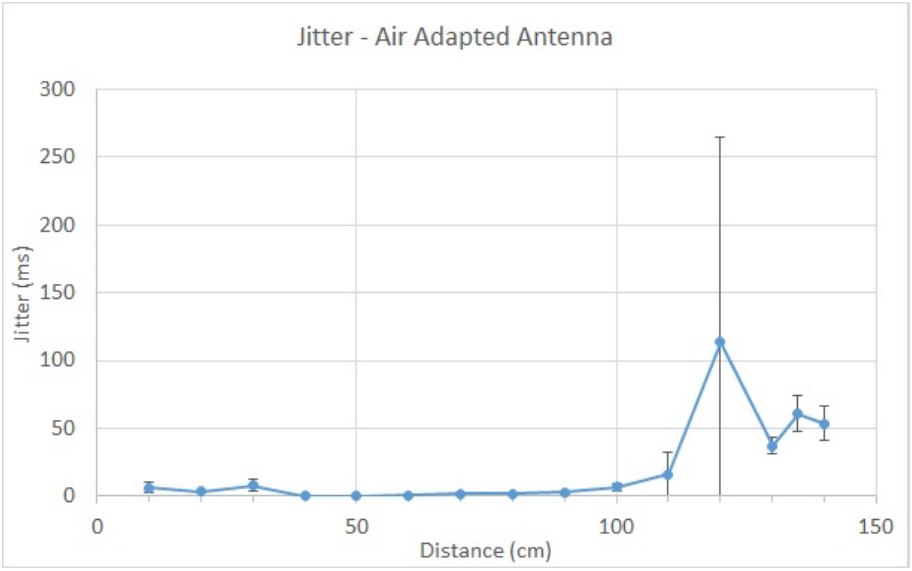

Figure 4.7: Jitter

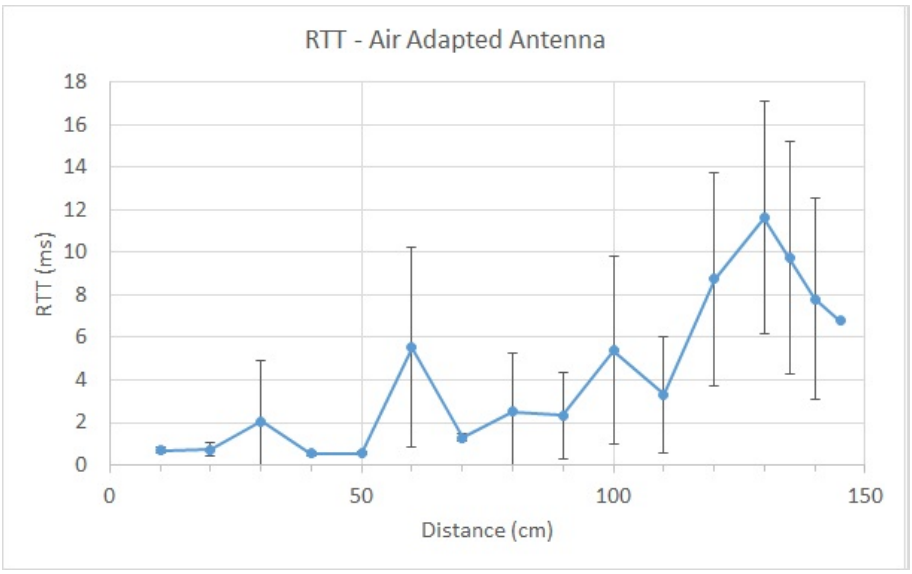

Figure 4.8: RTT

As for RTT, seen in Figure 4.8, we experienced some oscillations while increasing the distance. Represented by the confidence interval, we can see the same order variations in each distance. At the limit of the connection, a Round Trip Time of around 7 ms was observed. These values of RTT are considerably low, particularly if compared with acoustic links RTT which is higher.

4.1.1.2 With adaptation

In this Section we analyze the results obtained using the underwater adapted antenna.

- **Measured and Theoretical RSSI**

Figure 4.9 presents the results of the RSSI for the different distances. Similar to when the air adapted antenna was used, values of RSSI higher than -20 dBm are present but in this case until a distance of around 80 cm. From that point RSSI progressively decreases with small variations until 155 cm, point where RSSI begins to show higher variations. The last distance able to establish a communication was at 215 cm, with an RSSI value of approximately -63 dBm.

Again, the minimum signal received suggest that the wireless driver is not reporting correct values, and a -24 dB offset was applied to the results in order to properly compare to the theoretical models.

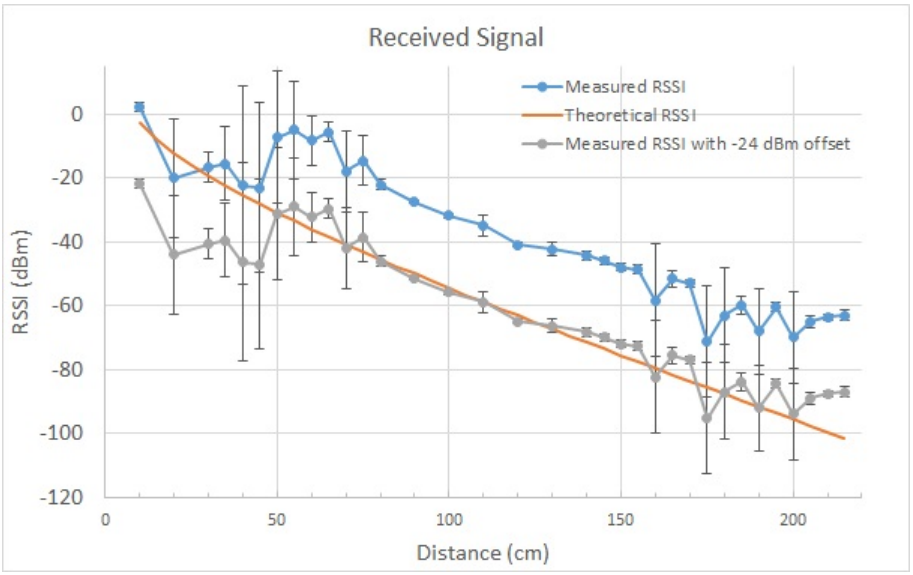

Figure 4.9: Measured vs Theoretical RSSI.

Theoretical values are now almost overlapping the experience results, if a -24 dBm is applied.

- **TCP and UDP Throughput**

Concerning Throughput experiments, these show similar results to the ones using the air adapted antenna. In fact, almost the exact same throughput values were observed but with a shift to higher distances and a longer maximum communication distance. The low throughput values are now detected until around the 70 cm distance. Throughput reaches 22 Mbit/s at the 90 and 100 cm mark, distance in which starts to lower progressively until the limit of communication. The last point recorded was at 210 cm with throughput of around 120 kbit/s. Comparing to the air adapted antenna, this represent an improvement of 50% in the maximum range distance. Again, the limitation of throughput can be explained by an excess of signal at the receiver or/and caused by near-field effects. In this case, the antenna has a diameter with 10 cm, thus, theoretically, near-field region reaches 46 cm.

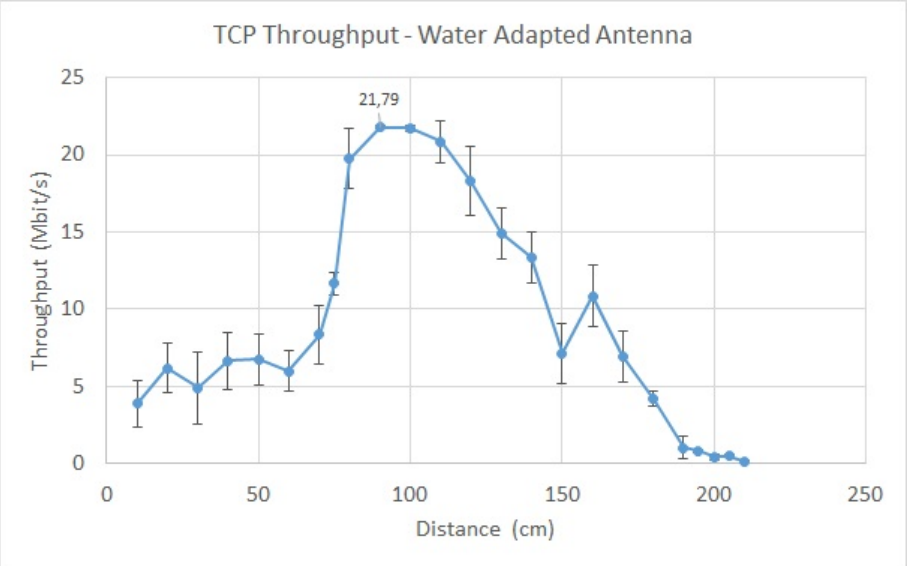

Figure 4.10: TCP Throughput

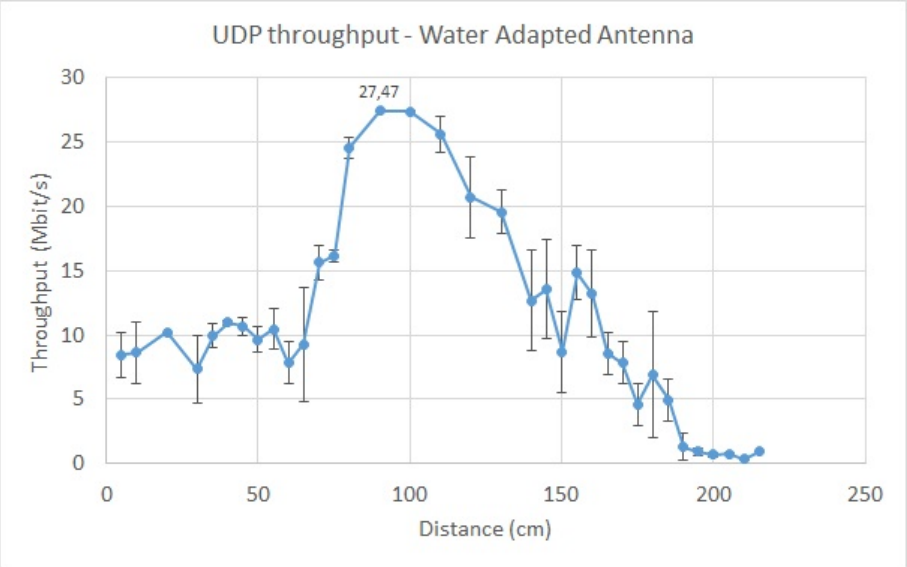

Figure 4.11: UDP Throughput

UDP Throughput shown in Figure 4.11 shares the same characteristics with the TCP results, but as with the previous antenna, with a global increase in the throughput for all the distances. A Throughput of 28 Mbit/s was experienced at 90 cm, and almost 1 Mbit/s at 215 cm.

- **Jitter and Round Trip Time**

  Figure 4.12 represents the measures of Jitter. As we can see, for distances up to 30 cm, high variations in the jitter were detected. From this distance on, lower than 10 ms jitter with no variations was observed for until 180 cm. Further from this point, we can see an increase in the jitter with bigger variations, reaching a maximum of around 100 ms at 210 cm.

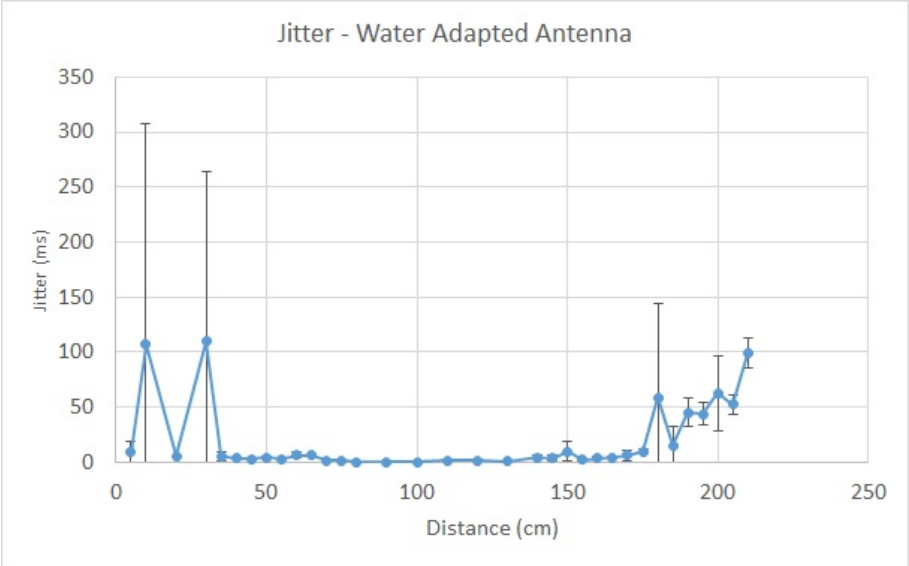

Figure 4.12: Jitter

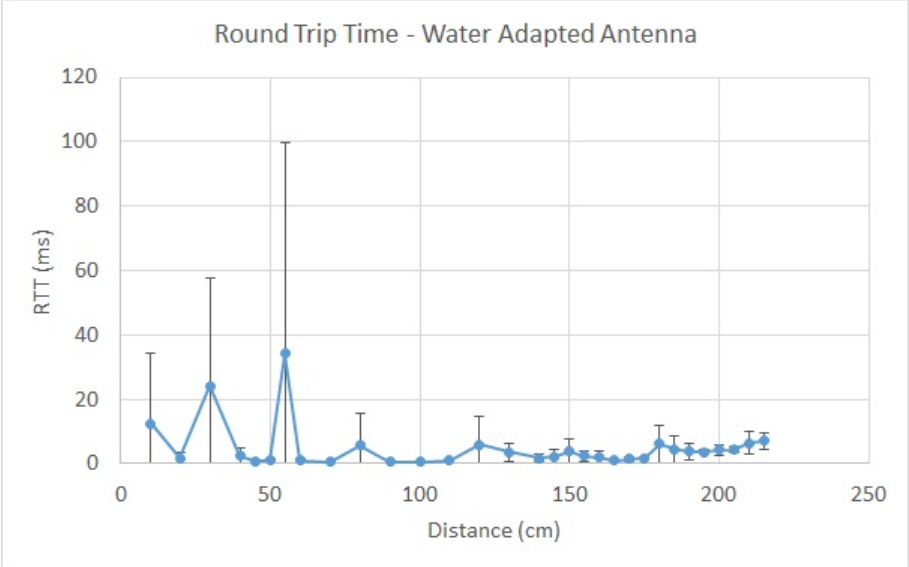

Figure 4.13: RTT

Figure 4.13 gather the results of the Round Trip Time. High oscillations in the signal are observed until the 70 cm mark, reaching maximum values of around 100 ms. After this, a stable behavior is maintained until the end of the communication distance, with values lower than 10 ms.

4.1.2 2.4 GHz

This Section refers to the experiments made using the RouterBoard r52-nM wireless card presented in Section 3.2.4.2, and the 2.4 GHz patch antenna shown in Section 3.3.2. For this case, the configurations can be viewed in Table 4.2. The channel used was 11 with a carrier frequency of 2.462 GHz. The choice of this channel was due to the good results in that frequency when

measuring the s11 parameter underwater for the 2.4 GHz patch antenna, as shown in Figure 3.23. A 40 MHz channel bandwidth was used to enable higher maximum throughput and TX power was set to the maximum possible of 19 dBm.

Table 4.2: Summarization of 2.4 GHz Link Configurations.

Link parameter	Value
Wireless Standard	802.11n
Network Mode	Ad-Hoc
Channel	11 (2.462 GHz)
Channel Bandwidth	40 MHz
TX Power	19 dBm
Bit rate	Auto
Noise level	-90 dBm
Pigtail and connectors Loss	< 2 dB
Antenna Gain	9 dBi

- **Measured and Theoretical RSSI**

  Figure 4.14 plots the RSSI obtained using the 2.462 GHz frequency. Starting at the 10 cm mark with -33 dBm, we can see a big difference if we compare to the values at 10 cm from the 768 MHz frequency tests. The signal then decreases with no oscillations, reaching a maximum link distance of 32 cm, with an average of -83 dBm.

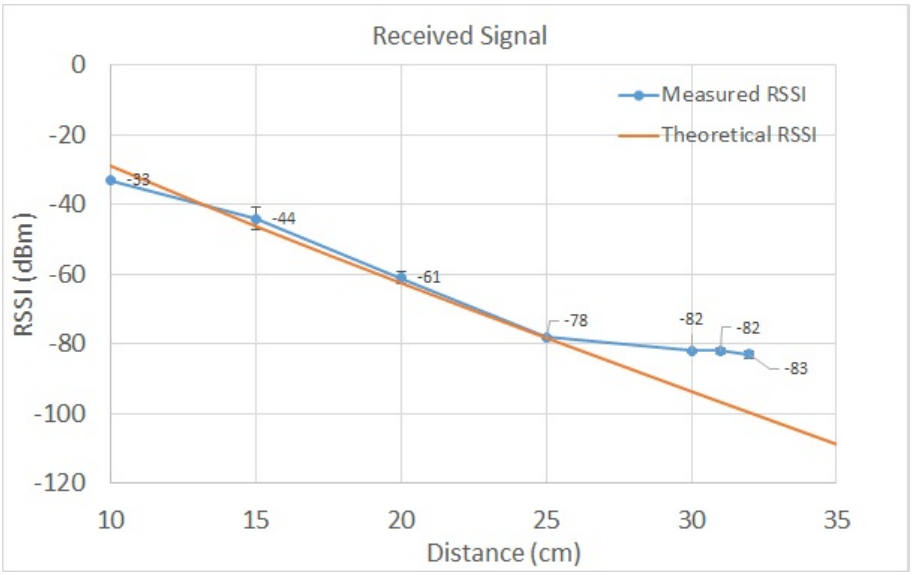

Figure 4.14: Measured vs Theoretical RSSI.

  Results show, again, identical values comparing to the theoretical model, with a higher difference being noticed after the 30 cm mark.

- **TCP and UDP Throughput**

Figure 4.15 shows TCP Throughput results. A maximum of around 107 Mbit/s was achieved and higher values than 100 Mbit/s were observed until 20 cm of distance. As seen in the figure, a strong decay in the throughput was experienced before reaching the distance limit, with approximately 700 kbit/s at 32 cm. UDP Throughput plotted in Figure 4.16 follows the same tendency but with small increase in each distance throughput. The results of 100 Mbit/s for distances until 20 cm, were limited by the Iperf UDP command where it was commanded a 100 Mbit traffic generation. This value could, although, reach higher values if a large bandwidth had been generated, possibly higher than 120 Mbit/s.

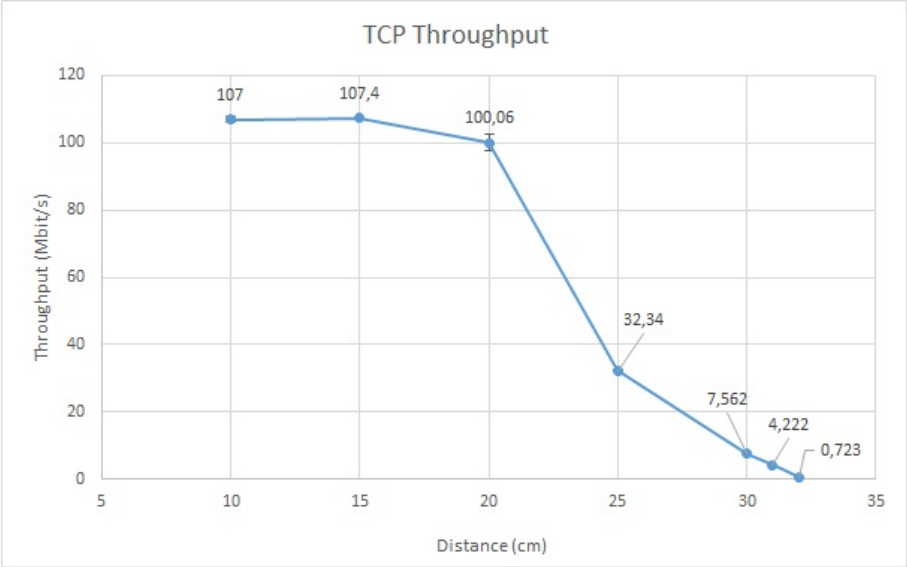

Figure 4.15: TCP Throughput

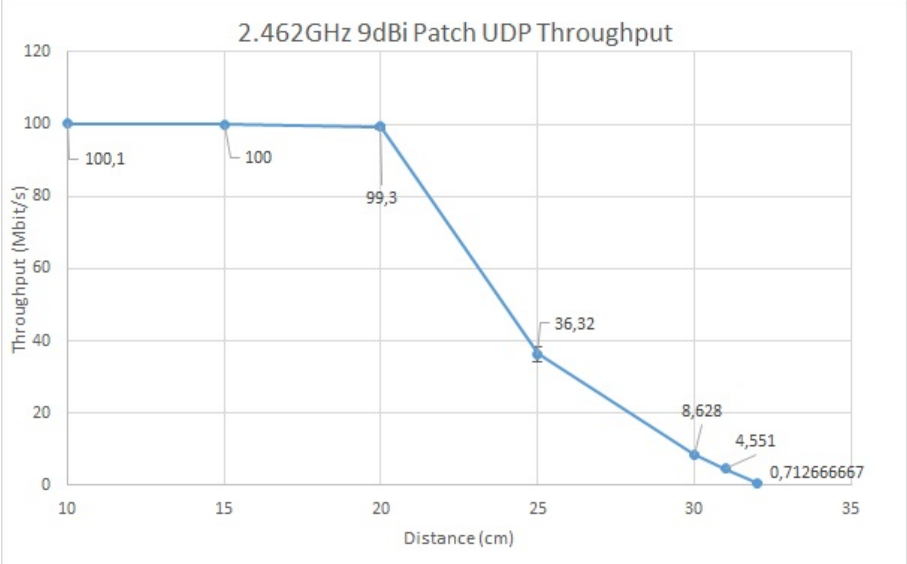

Figure 4.16: UDP Throughput

- **Jitter and Round Trip Time**

Very low jitter was experienced in 2.4 GHz, except for the last point of communication range. As seen in Figure 4.17, a maximum of 6.5 ms of jitter was recorded until the distance of 31 cm. At 32 cm a high average and strong variations can be observed, at a distance where RSSI was extremely low.

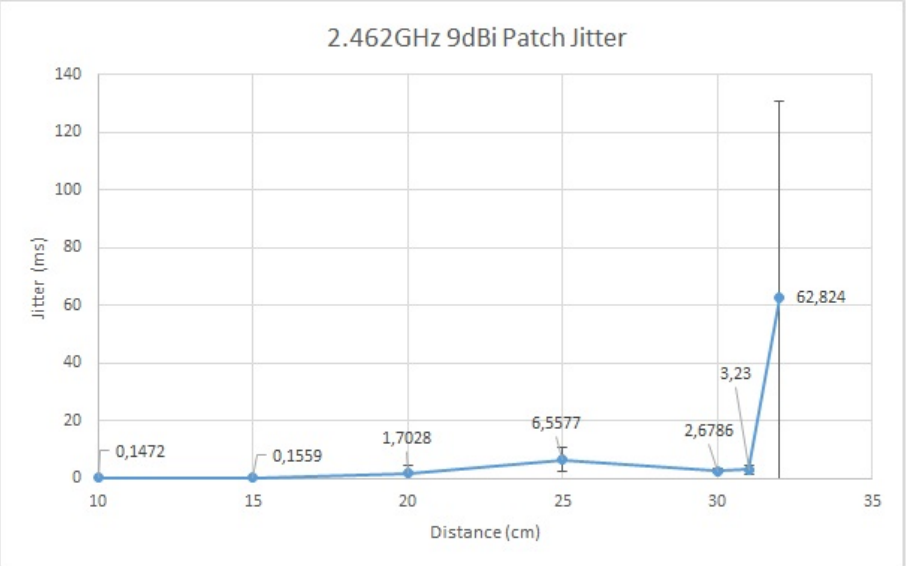

Figure 4.17: Jitter

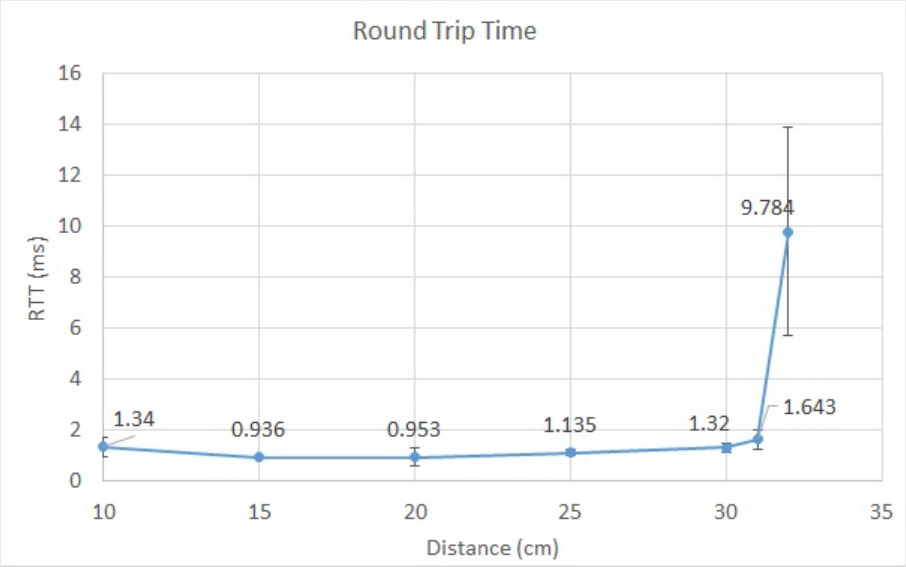

Figure 4.18: RTT

Round Trip Time performed similarly, with very good values until 31 cm and strong variations at 32 cm.

4.1.3 5 GHz

The channel used for the 5 GHz band was channel 48 with a frequency of 5.24 GHz, because it provided the best power efficiency for our underwater environment. A summarization of the link parameters are present in Table 4.3. As theoretical propagation models suggest, the water attenuation using such a high frequency as 5 GHz results in a very low communication range. In fact, using our setup, only 10 cm was reached before communication link dropped. Only two distances were measured being the closest 7.5 cm and the second 10 cm. At the time of the experiences it wasn't possible to bring the mobile node closer to the static one, because the lead plates were slightly positioned to the front of the node, in order to compensate the lack of weight in both the nodes fronts and provide a better parallelism.

Table 4.3: Summarization of 5 GHz Link Configurations.

Link parameter	Value
Wireless Standard	802.11n
Network Mode	Ad-Hoc
Channel	48 (5.240 GHz)
Channel Bandwidth	40 MHz
TX Power	19 dBm
Bit rate	Auto
Noise level	-95 dBm
Pigtails and connectors Loss	< 2 dB
Antenna Gain	15 dBi

- **Measured and Theoretical RSSI**

Figure 4.19 shows RSSI results for the two measured distances. A fast drop in signal can be observed, reducing from -74.6 dB to -85 dB in only 2.5 cm.

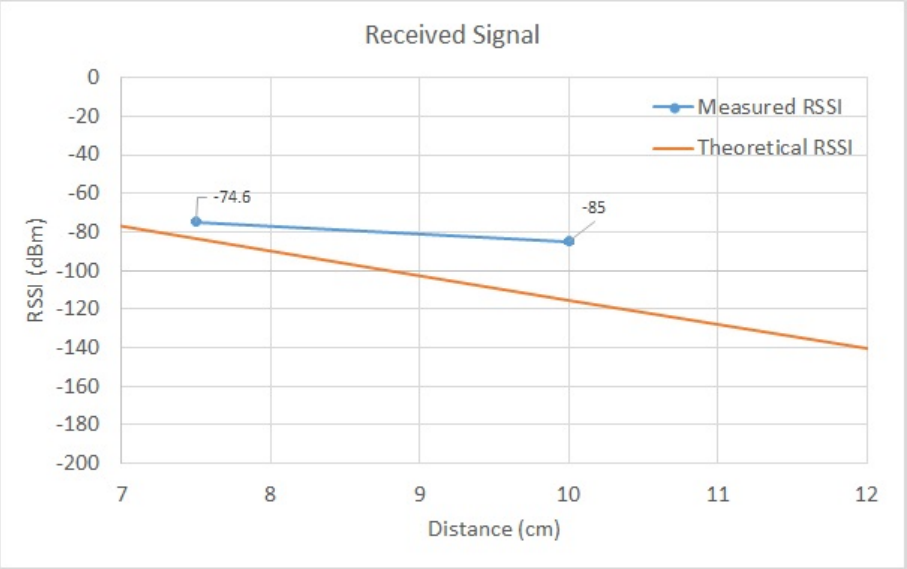

Figure 4.19: Measured and Theoretical RSSI.

Theoretical models suggest a higher attenuation that the experienced results but due to the low amount of distances evaluated and how small imprecisions affect RF attenuation at this frequency, we do not believe a good comparison can be performed.

- **TCP and UDP Throughput**

Figures 4.20 and 4.21 provide TCP and UDP Throughput results. As in concordance with Throughput measures using the previous frequencies, both parameters have similar behaviors showing again the slight increase when using UDP. The results indicate a Throughput of 11.27 Mbit/s for TCP at the limit of communication while 13.28 Mbit/s for UDP. Although only a short range is possible, we consider these throughputs high enough to benefit certain applications that are able to achieve this proximities between devices.

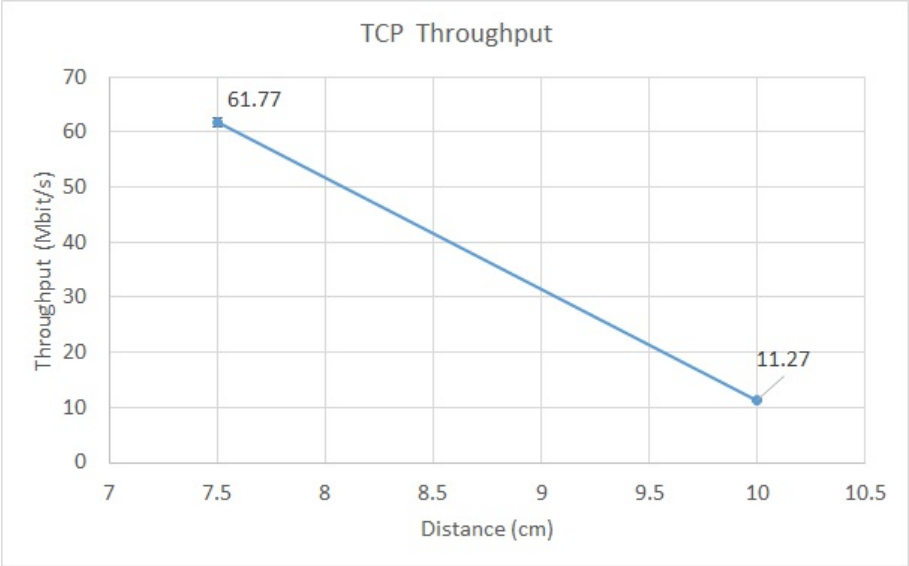

Figure 4.20: TCP Throughput

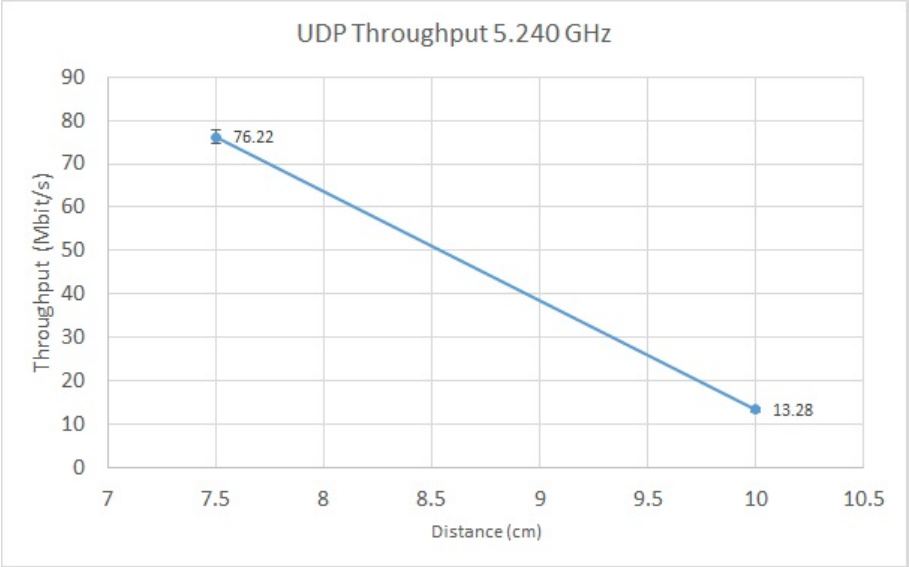

Figure 4.21: UDP Throughput

- **Jitter and Round Trip Time**

As for the Jitter, Figure 4.22 shows that some high delay peaks were experienced at the 7.5 cm distance, making the average higher than the 10 cm mark. At the communication limit of 10 cm the measured value was 2.7 ms.

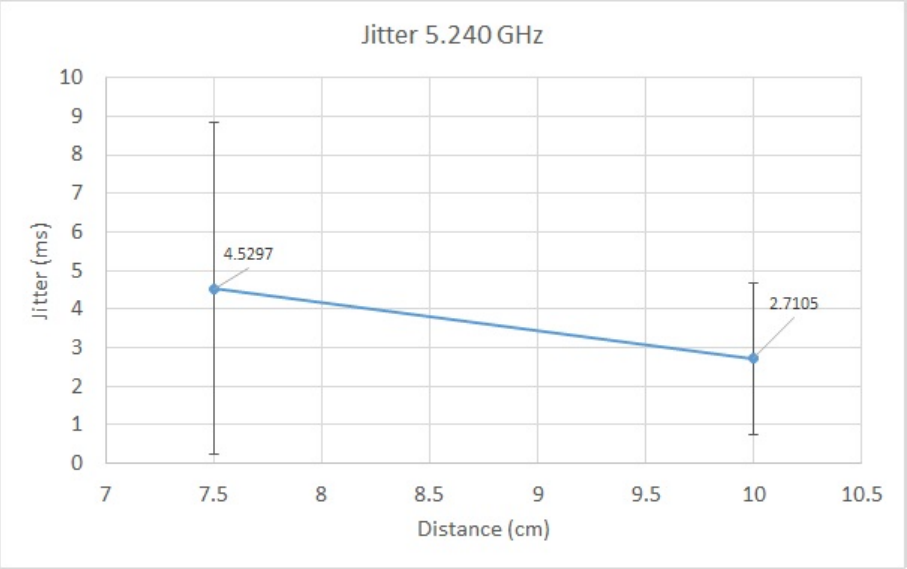

Figure 4.22: Jitter

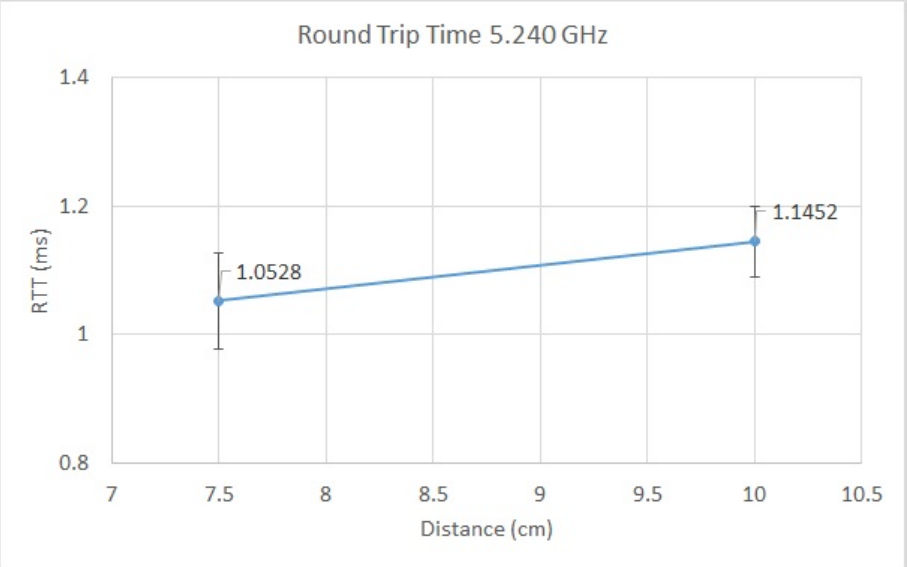

Figure 4.23: RTT

Figure 4.23 shows that Round Trip Time remained low and stable for both distances.

4.2 Multiple Access Performance Evaluation

Multiple Access evaluation was implemented using the 2.4 GHz band frequency. The same test would be possible in the 770 MHz band but this would be highly susceptible to imprecisions if implemented with our setup and would involve more logistics requiring a great amount of time. All the link parameters were kept from the previous 2.4 GHz point-to-point evaluations. In this case, a node was chosen as Access Point, while the other two nodes configured as stations. Figure 4.24 provides a real picture of this setup, where the node to the right is the Access Point.

Because of the dimensions of the waterproof case, the minimum distance able to be measured was 15 cm, from the Access Point to each of the stations. From there, distances 20, 25 and 27 cm were measured. Although a 30 cm distance was possible in the Point-to-Point setup, because of the angle the nodes were making with the Access Point, this was receiving less signal, as the radiation pattern of the 2.4 GHz patches suggest.

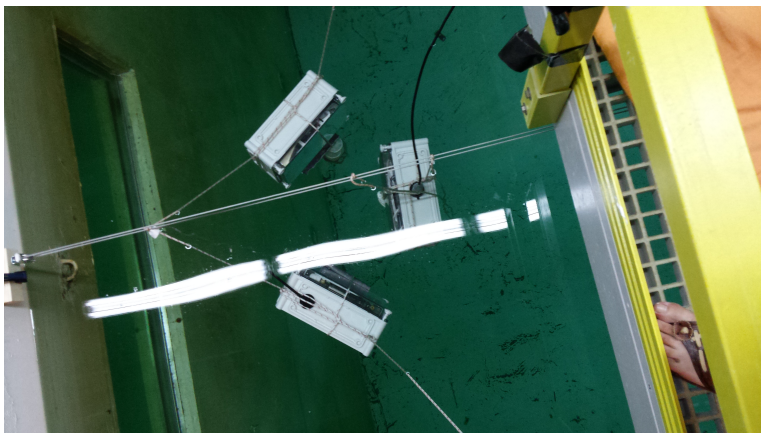

Figure 4.24: 3 Nodes Multiple Access Evaluation Setup

At each distance, an Iperf connection was established between each node and the Access Point. First, TCP and UDP performance was measured one node at a time, so we could see the throughput each node could achieve without the interference of the other. Then, throughput was measured while both nodes communicate with the Access Point. These throughputs were recorded and added to represent the combined throughput. The goal here is to understand at witch distance multiple access mechanisms cannot correctly intervene, because one node does not know the other is already sending packets to the Access Point. Figure 4.25 shows Throughput results for simultaneous and separate connections.

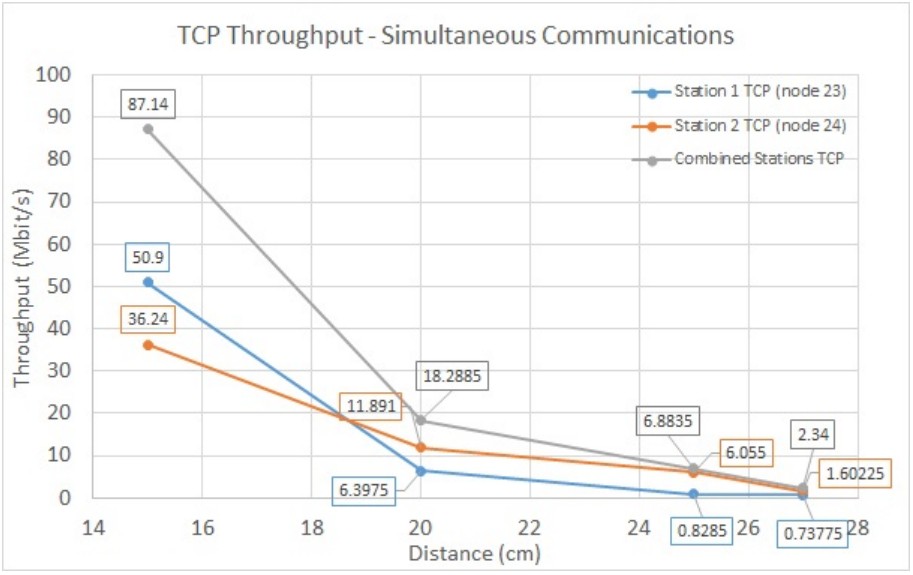

(a) Simultaneous Throughput

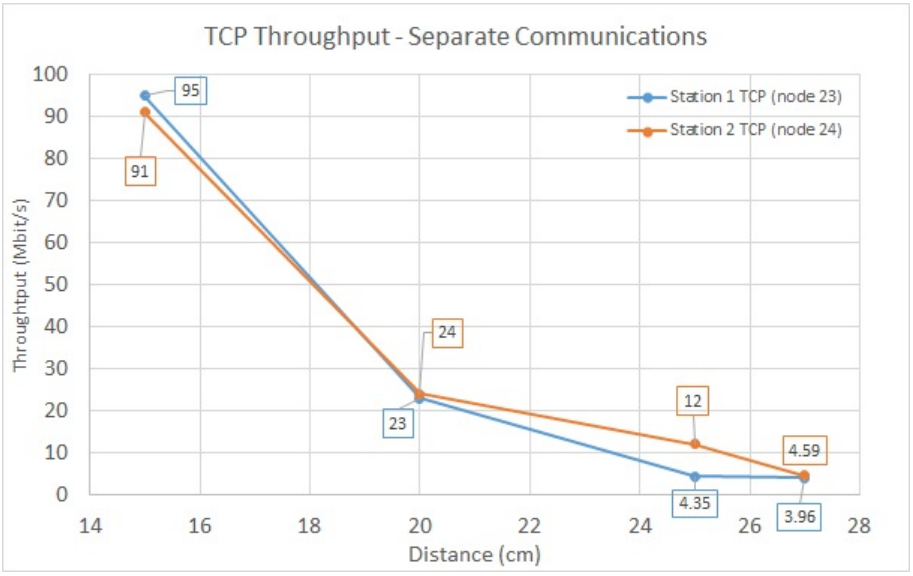

(b) Separate Throughput

Figure 4.25: TCP Throughput using 3 nodes.

Figure 4.25b suggests Station 2 link conditions with the Access Point were generally better. The highest difference was observed on the 25 cm mark, with 12 Mbit/s for Station 1 and 4.35 Mbit/s for Station 2. Although a big effort was made in order to give each node the same conditions to transmit, the setup was sensible for imprecisions.

Analyzing the results of both figures, and if we make a comparison between the Combined throughput when the nodes transmit at the same time versus the separate throughput of the node in the best condition, we see a clear degradation evolution of the simultaneous transmissions with the increase in the distance. At a distance of 15 cm the Combined Throughput is 87 Mbit/s, while a 95 Mbit/s was experience using a separate transmission. Converting this difference into % of

throughput lost, we have around 9% less throughput. At 20 cm Combined Throughput is 18.3 Mbit/s and separate achieves 24 Mbit/s, resulting in around 24% less throughput. At 25 cm we have a combined throughput of 6.9 Mbit/s. Since separate is 12 Mbit/s, we now have a 43 % loss. Finally, at 27 cm the combined throughput is 2.34 Mbit/s and separate 4.6 Mbit/s resulting in around 50% less throughput.

These results show that an acceptable fairness is observed until the 20 cm mark, where some throughput loss was experienced due to medium competition. From this distance on, the reduction of combined throughput highly increases, and starvation of Station 1, evidenced by its throughput of 0.8285 Mbit/s versus 6 Mbit/s of Station 2 at the 25 cm mark, imply the presence of the Hidden Node, where Stations can not hear each other.

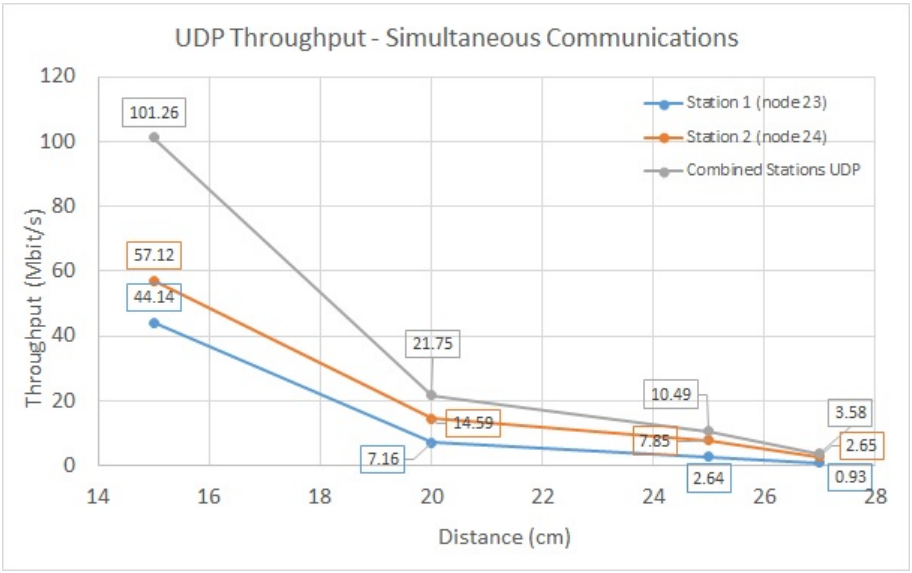

(a) Simultaneous Throughput

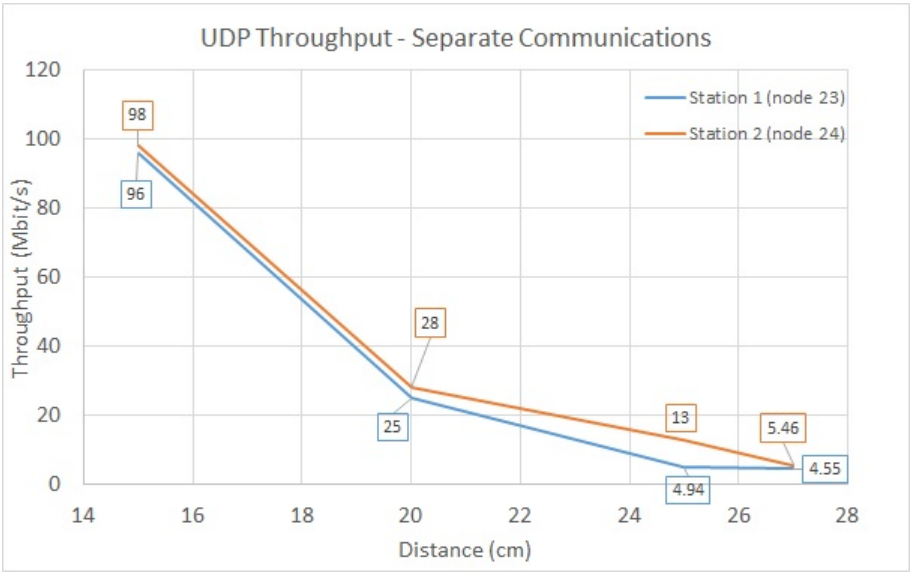

(b) Separate Throughput

Figure 4.26: UDP Throughput using 3 nodes.

Figure 4.26a and 4.26b provide UDP communication results. Same conclusions as in the TCP throughput case can be retrieved, with a small overall increase in throughput. At the maximum range of 27 cm between each node and the Access Point, Station 1 shows strong starvation with less than 1 Mbit/s versus 2.65 Mbit/s of Station 2, when both nodes are transmitting. A decrease in throughput of around 35 % can be observed when comparing combined throughput and highest throughput of Station 2 (5.46 Mbit/s).

A mechanism created to reduce this effect is RTS/CTS. If enabled on a particular station, it will refrain from sending a data frame until the station completes a RTS/CTS handshake with another station, such as an access point, thus avoiding collisions.

4.3 Discussion

In this section we discuss the performance results achieved within the 768 MHz, 2.4 GHz and 5 GHz band. In the 768 MHz band, the results using the air adapted and water adapted antennas are compared as for the results obtained in the 2.4 and 5 GHz band using patch antennas. We further discuss the 3 node Multiple Access evaluation performance results.

Regarding the 768 MHz band, when the air adapted antenna was used to test the performance and a limitation in throughput was observed for close distances, there was the possibility of this being caused by either a excess of power arriving at the receiver or the occurrence of a near-field effect. Comparing the results of the RSSI and Throughput of both antennas we can see that the limitation of throughput occurs, in both cases, when the RSSI is above -20 dB. This might prove the excess of power at the receiver as one of the causes of the limitation. Moreover the decrease in throughput was also experimentally observed in over-the-air communications with the receiver being in the far-field region, thus near-field effects were not present. Also, since the wavelength underwater is in the order of 4 cm, near-field effect may be occurring, thus helping in the degradation of the received signal. To avoid these effects, lower transmitting powers could be used and also, the use of other antennas, with dimensions shorter than half of the wavelength of the radiation they emit, could greatly reduce the distance at which near-field effects deteriorates the communication link. For such antennas, the far-field becomes the region at a distance of 2λ, in this case, 8 cm.

Performance evaluation in 768 MHz using the air adapted antenna resulted in a maximum communication distance of 140 cm, while the adaptation of the antenna provided to the setup a distance of 210 cm. The behavior of all the performance parameters measured using both antennas were very similar apart from the increase in the range. These results lead to an improvement in range of 50%. We consider this is an innovative achievement and similar results are not found in other related articles. Ranges of 2 meters with throughputs with a minimum of 1 Mbit/s provide quality video transmission in real time. Jitter and RTT were low and similar to the ones experienced in over-the-air communications, being able to satisfy the requirements of any existing or future application.

When working at the 2.4 GHz band frequency, more precisely at 2.462 GHz, with a 40 MHz channel, performance metrics show stable results but a communication range of only 32 cm. A lot less range was achieved comparing to simulation results in [31], where the maximum distance of communication is about 1.4 meters. Although 802.11g standard was used in this simulation, both throughput curves show similar behaviors, with a constant throughput zone followed by a rapid decrease. Being our antenna in contact with the air, medium transitions and the actual testbed may introduce losses that are not considered in the simulation. A slight improvement was achieved comparing to other publications of practical experiments using this frequency. In [7], a maximum distance of 17 cm was achieved using a BPSK modulation of 1 Mbit/s. A better result was achieved in [32], with a maximum range of 26 cm, at frequency 2.427 GHz, OFDM modulation and 12 Mbit/s data rate. Ranges achieved in this dissertation could, for example, be used to design an underwater Wi-Fi zone, where devices could periodically upload/download data at high data rates and then resume their journeys.

Underwater communications using 5 GHz band frequencies resulted, in our setup, in a 10 cm maximum communication distance. Throughputs achieved of 11 Mbit/s are interesting and may well suit a system where physical contact between devices is possible.

Results obtained provided a validation of theoretical models for the frequencies in evaluation, evidencing the feasibility of the testbed.

Finally, Multiple Access performance evaluation allowed to understand how these mechanisms behave when two concurrent nodes try to transmit to the same receiver at the same time, when the distance between them is increased. At 25 cm, from the stations to the Access Point, distance between stations was around 35 cm. At this point the Hidden Node Problem manifested since one of the stations entered starvation. This because stations stopped detecting each other and CSMA/CA mechanism could not avoid collisions at the Access Point. RTS/CTS mechanism may provide increased performance if enabled in this environment characterized with such high attenuations and where the Hidden Node Problem is more likely to happen.

Chapter 5

Conclusions and Future Work

New emerging underwater applications are demanding new technologies that provide high data rates allied with low acquisition and maintenance costs. Acoustic and Optical solutions may not be a solution for many of these applications. The use of electromagnetic propagation underwater has been avoided since the early days of amateur radio, due to the high attenuation theoretical models predict.

In this MSc thesis, underwater Wi-Fi communications using 700 MHz, 2.4 GHz and 5 GHz bands are evaluated. Experimental results show that using low frequencies such as 768 MHz it is possible to achieve acceptable distances and data rates. The new antenna developed for 768 MHz underwater provided an improvement of 50% in range, allowing communications at 2.1m with a throughput of 130 kbit/s. We believe many applications could benefit from this low cost 2 meter range Wi-Fi solution. This solution could, per instance, provide to an underwater structure a Personal Area Network, possibly linking devices with common tasks or roles, while isolating them from other devices or undesired listeners.

Regarding the 2.4 GHz frequency, an increase of at least 35% in the maximum range was experienced considering other related experimental publications. Although with a maximum range of 32 cm, we think it is able for scenarios where existing Wi-Fi hardware is present, as in most AUVs/ROVs. Uploading/Downloading Wi-Fi zones can be deployed with this technology, allowing devices to rapidly exchange information without requiring much alignment.

As for 5 GHz band frequencies, a maximum distance of 10 cm was experienced. The throughput of 10 Mbit/s achieved with this range is high enough to satisfy most applications data rate requirements. Although almost a physical contact between devices is needed, this could be used to give birth to a new type of underwater connectors. These could be used, for example, to attach modules with different functions to an underwater structure. This would eliminate the need for transmission cables thus avoiding compromising the structure's waterproofing.

The limited ranges achieved also represent that communications underwater may be characterized by an extreme level of security in a way that undesired interceptions of the transmission will be impeded by high attenuations.

Theoretical models proved to be valid for the results obtained with our setup. This also evidenced the robustness of the implemented testbed.

As in over-the-air, Multiple Access communications in underwater scenarios show the Hidden Node Problem, and collisions strongly reduce the transmission performance. This effect may be even more stimulated by the strong attenuation in underwater environments and mechanisms that aim to reduce it, like RTS/CTS, may highly improve underwater networks.

We finally conclude that the underwater environment is full of challenges. Being in the presence of a unstable medium where imprecise variables affect water behavior towards radio frequency and how small changes to these affect wireless communications performance, imply that each specific scenario demands its own underwater communications design and optimization.

5.1 Future Work

Although we finish this thesis with a sense of accomplishment, we know there are many improvements to be made regarding Wi-Fi underwater communications:

- **Wi-Fi performance evaluation using antennas in contact with water** - This thesis performance results were achieved including the antenna inside the node. When transmitting from a node to another, electromagnetic waves had to go through different types of mediums (air, case material and water). These transitions may affect the quality of the signal arriving at the receiver. Thus, we think an evaluation using antennas in contact with the water should be carried in the future.

- **New methods to test underwater antennas -** As theoretical models and spectrum analysis on submerged antennas might provide good characterizations, new methodologies and devices, such as underwater anechoic chambers could extremely enrich this knowledge.

- **Working in lower frequencies -** The good results obtained when working in a lower frequency, show that if communications in even lower frequencies are permitted and followed by compatible hardware, it is possible to achieve even higher distances using electromagnetic waves.

- **Auto Rate Mechanisms for underwater scenarios -** Although the modulations in use at each distance of evaluation are not present in this thesis, these show that some improvements could be made to the Automatic Rate Adaptation mechanisms. On almost every distance evaluated, modulations used were very high comparing to the actual throughput of the transmission. A better synchronization between RSSI and data rate could provide better results.

- **Multiple Access evaluation on 700 MHz -** In this thesis, the performance of Multiple Access was tested in 2.4 GHz without enabling RTS/CTS mechanism. This mechanism is a supplement to CSMA/CA that aims to reduce frame collisions introduced by the hidden

node problem. In the future, performance tests using this mechanism should be carried and compared to results achieved in this dissertation. The same applies to the 700 MHz frequency, which frequency was not evaluated in this thesis, regarding Multiple Access.

References

[1] Shan Jiang. Electromagnetic Wave Propagation into Fresh Water. *Journal of Electromagnetic Analysis and Applications*, 03(07), 2011.

[2] Bridget Benson. *Design of a lowcost underwater acoustic modem for short-range sensor networks*. PhD thesis, University of California, San Diego, 2010.

[3] Heather Brundage. Designing a Wireless Underwater Optical Communication System. Master's thesis, Massachusetts Institute of Technology, 2010.

[4] Milica Stojanovic. Underwater Acoustic Communications: Design Considerations on the Physical Layer. *2008 Fifth Annual Conference on Wireless on Demand Network Systems and Services*, (2), January 2008.

[5] Shijian Tang, Yuhan Dong, and Xuedan Zhang. On Link Misalignment for Underwater Wireless Optical Communications. *IEEE Communications Letters*, 16(10), October 2012.

[6] X. Che, I. Wells, G. Dickers, P. Kear, and X. Gong. Re-evaluation of RF electromagnetic communication in underwater sensor networks. *IEEE Communications Magazine*, 48(12), 2010.

[7] Sandra Sendra, Jose V. Lamparero, Jaime Lloret, and Miguel Ardid. Underwater Communications in Wireless Sensor Networks using WLAN at 2.4 GHz. *2011 IEEE Eighth International Conference on Mobile Ad-Hoc and Sensor Systems*, October 2011.

[8] Alejandro Palmeiro, Manuel Martin, Ian Crowther, and Mark Rhodes. Underwater radio frequency communications. *OCEANS 2011 IEEE - Spain*, 2011.

[9] I Wells, A Davies, X. Che, P. Kear, G. Dickers, X. Gong, and M. Rhodes. Node pattern simulation of an undersea sensor network using rf electromagnetic communications. In *Ultra Modern Telecommunications Workshops, 2009. ICUMT '09. International Conference on*, pages 1–4, Oct 2009.

[10] Michael R. Frater, Michael J. Ryan, and Robin M. Dunbar. Electromagnetic communications within swarms of autonomous underwater vehicles. In *Proceedings of the 1st ACM International Workshop on Underwater Networks*, WUWNet '06, pages 64–70, New York, NY, USA, 2006. ACM.

[11] Seatooth® S300 Through water Radio Modem. Wireless For SubSea. Accessed: 2013-02-10. URL: http://www.wfs-tech.com/images/uploads/Seatooth_S300_13_10.pdf.

[12] C. Uribe and W. Grote. Radio communication model for underwater wsn. In *New Technologies, Mobility and Security (NTMS), 2009 3rd International Conference on*, Dec 2009.

[13] Ali Elrashidi, Abdelrahman Elleithy, Majed Albogame, and Khaled Elleithy. Underwater Wireless Sensor Network Communication Using Electromagnetic Waves at Resonance Frequency 2.4 GHz. Department of Computer Science and Engeneering. University of Bridgeport. 2012.

[14] Lloyd Butler Vkbr. Underwater Radio Communication. *Amateur Radio*, (April), 1987.

[15] Mark Hoferitza. Radio waves : how RF technology can be used to form a wireless network under water. AustriaMicrosystems AG.

[16] Adriana B. Flores, Ryan E. Guerra, and Edward W. Knightly. IEEE 802.11af : A Standard for TV White Space Spectrum Sharing. Rice University. 2013.

[17] IEEE 802.11af project. Accessed: 2013-05-10. URL: http://grouper.ieee.org/groups/802/11/Reports/802.11_Timelines.htm.

[18] XTREMERange7 700MHz WiFi radio module. UBIQUITI. Accessed: 2013-02-10. URL: http://dl.ubnt.com/xr7_datasheet.pdf.

[19] INESC TEC Robotics Facilities at ISEP. Accessed: 2013-05-10. URL: http://www.lsa.isep.ipp.pt/.

[20] WTW Inolab Cond Level I. Accessed: 2013-05-10. URL: http://www.geminibv.nl/labware/wtw-inolab-ph-level-1/wtw-cond-level1-manual-eng.pdf.

[21] Fibox EKJVT130T. Accessed: 2014-04-05. URL: http://catalogs.fibox.com/catalogs/pdf_productcard.pl?pr_id=990&lang_code=ENG1.

[22] American National Standard for Degrees of Protection Provided by Enclosures (IP Code). NEMA. Accessed: 2014-04-05. URL: https://www.galco.com/techdoc/wieg/pb4_ts.pdf.

[23] PC Engines alix3d3 System Board. Accessed: 2013-02-10. URL: http://pcengines.ch/alix3d3.htm.

[24] RouterBOARD R52n-M 802.11a/b/g/n dual band miniPCI card. MikroTik. Accessed: 2013-02-10. URL: http://i.mt.lv/routerboard/files/R52n-M.pdf.

[25] OpenWrt Linux distribution. Accessed: 2013-02-10. URL: https://openwrt.org/, arXiv:/openwrt.org/.

[26] David M. Pozar. Microwave Engeneering 4th Edition. 2011.

[27] Silva Santos Luciano. Wi-Fi Maritime Communications using TV White Spaces, 2013.

[28] StationBox Mikro. Accessed: 2014-04-05. URL: http://www.stationbox.info/StationBoxMikro.html.

[29] Hector Fabian Guarnizo Mendez, Francois Le Pennec, Christian Gac, and Christian Person. Deep underwater compatible Wi-Fi antenna development. *2011 The 14th International Symposium on Wireless Personal Multimedia Communications (WPMC)*, pages 1–5, 2011.

[30] C.W. Wang and T. Keech. Antenna Models For Electromagnetic Compatibility Analyses. U.S. DEPARTMENT OF COMMERCE - National Telecommunications and Information Administration, 2012.

[31] Filipe Teixeira, Rui Campos, and Manuel Ricardo. Performance Evaluation of IEEE 802.11 Underwater Wireless Networks. In procedings of the 13rd Conferencia de Redes de Computadores (CRC2013), November, 2013.

[32] S Sendra, J Lloret, J.J.P.C. Rodrigues, and J M Aguiar. Underwater Wireless Communications in Freshwater at 2.4 GHz. *Communications Letters, IEEE*, 17(9), 2013.